Chapter 6

NAPHTHALENE AND ANTHRACENE BASED FUSED-RING COMPOUNDS WITH NLO PROPERTY

6.1 Introduction:

The strategy behind this work was to increase π-donor strength with a splendid source of π-electrons, as naphthalene and anthracene replacing phenyl ring B, commonly used in the donor end of the main conjugation. Moreover, these fused ring systems were substituted with $-OCH_3$ and $-CH_3$ to study the structure-property relationship between the fused ring chalcones and two-photon absorption coefficient.

A series of eleven naphthalene-based chalcone derivatives, which can be further divided into three subseries according to the substituent present in the naphthalene skeleton, have been synthesized. Biological activity like antifungal and antibacterial activities of compounds consisting of naphthalene ring and heterocyclic ring have been reported by many research groups.[1-4] A series of fifteen anthracene-based chalcone derivatives, which can be further divided into three subseries as there are three different groups in the 9 position of the anthracene skeleton, have been synthesized. Some reported chalcones containing anthracene moiety have been observed to show fluorescence activity, photophysical and electrochemical properties [5, 6]. Polycyclic aromatic molecules like anthracene are used to prepare sensors for anions such as pyrophosphate, which is a useful fluorescent tool [7].

The general structure of these compounds can be categorized into two basic structural families of $D - \pi - A - D$ and $A - \pi - A - D$. Results are presented with a systematic effort to establish a relation between nonlinear absorption coefficients and the anthracenyl chalcone derivative. Nonlinear optical materials with fused ring (naphthalene and anthracene) chalcone derivatives have not been explored till now.

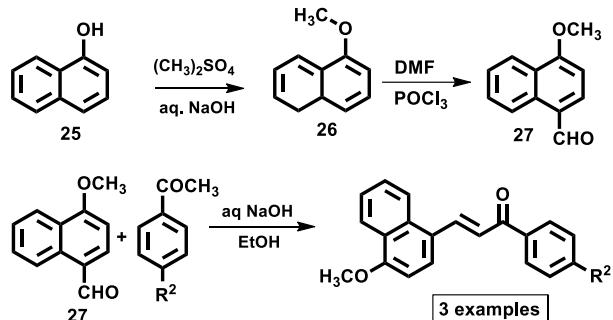## 6.2 Synthesis of Naphthalene Core Chalcone Derivatives:

2-methoxynaphthalene (**23**) and 1-methoxynaphthalene (**26**) was synthesized through methylation of *ß*-naphthol (**22**) and *α*-naphthol (**25**) respectively with dimethyl sulfate. 1-methoxy-4-naphthaldehyde (**27**) and 2-methoxy-1-

naphthaldehyde (**24**) was obtained through formylation of **26** and **23** respectively with DMF and POCl₃ in good yield. The Scheme for the preparation of compounds **22-27** [8] and naphthalene core chalcones are shown in Scheme 6.1.
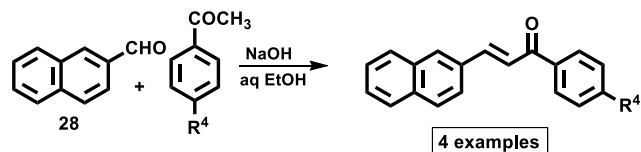
Synthesis of 1-(4-substitutedphenyl)-3-(1-methoxynaphthalen-2-yl)prop-2-en-1-one
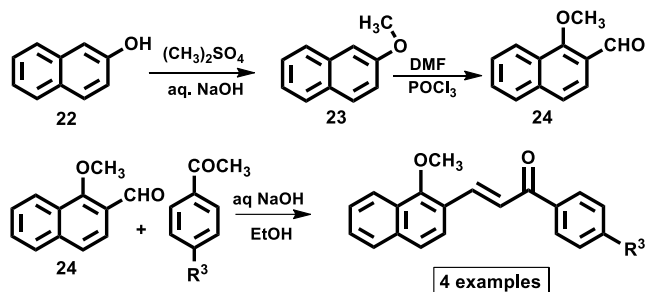
Synthesis of 3-(4-methoxynaphthalen-1-yl)-1-(substitutedphenyl)prop-2-en-1-one

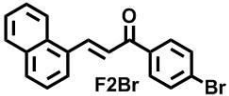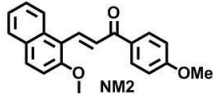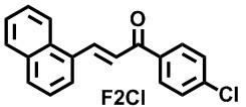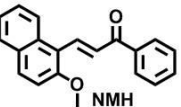**Synthesis of 1-(4-substitutedphenyl)-3-(naphthalen-2-yl)prop-2-en-1-one**
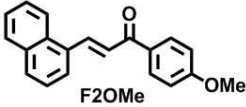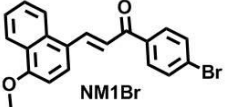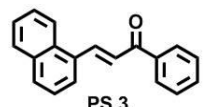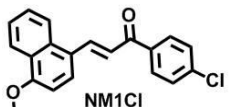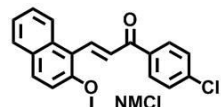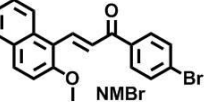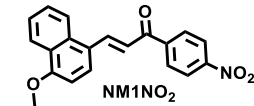
Scheme 6.1: Synthesis of naphthalene core chalcone derivatives.

6.2.1 General procedure of naphthalene core chalcone derivatives:

A solution of NaOH (40% w/v) in ethanol and water was prepared and placed in an ice bath, acetophenone (1 mmol) was added to this solution. After 15-20 min aldehyde derivative (1 mmol) was added. After complete addition, the reaction mixture was warmed. The reaction temperature was maintained at 38-40˚C. It was stirred for an appropriate time, Table 6.1 incorporates the reaction time and physical

data of the synthesized chalcone derivatives. The reaction mixture was refrigerated overnight. The reaction mixture was poured onto crushed ice and acidified with conc. HCl; precipitate obtained was filtered, washed with water till the pH was neutral. The product was dried and recrystallized with ethanol.

Table 6.1: Reaction time and Physical data of naphthalene core chalcone derivatives.

Compound & code	Time	M.P. (℃)	Compound & code	Time	M.P. (℃)
F2Br	3 h	174-176	NM2	30 h	137-139
F2Cl	10 h	159-161	NMH	15 h	108-110
F2OMe	5 h	169-171	NM1Br	24 h	110-112
PS 3	4 h	145-147	NM1Cl	24 h	109-110
NMCl	7 h	108-109	NMBr	12 h	110-112
NM1NO$_2$	5 h	130-132			

6.3 Characterization of naphthalene core chalcone derivatives:

^{1}H NMR **(400 MHz)** spectrum of *(E)-1-(4-bromophenyl)-3-(2-methoxynaphthalen-1-yl)prop-2-en-1-one* (**NMBr)** in CDCl$_3$ solvent is shown in Fig. 6.1, the structure in Fig. 6.1a and Fig. 6.2 displays the region δ 7.2-8.6 ppm. A singlet at δ = 4.06 is observed for three H^c protons of the methoxy group. A doublet with J = 16 Hz, centered at δ = 8.50 ppm is observed for H^a proton, another doublet with J = 16 Hz, centered at 7.84 ppm is observed for H^b proton, this confirms the *trans* configuration of the compound. Fig. 6.3 contains the ^{13}C NMR (CDCl$_3$) spectrum of **NMBr**. δ = 190.22 for the carbonyl carbon, δ = 157.23 for the carbon on the naphthalene ring attached to the methoxy group. **NMBr** is taken as a representative compound from the series of naphthalene core chalcone derivatives. The other spectral data are tabulated below and spectra are available in the Section 6.12.
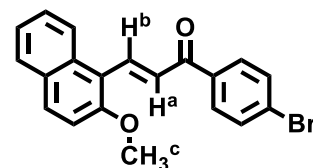
Figure 6.1a: Structure of NMBr.
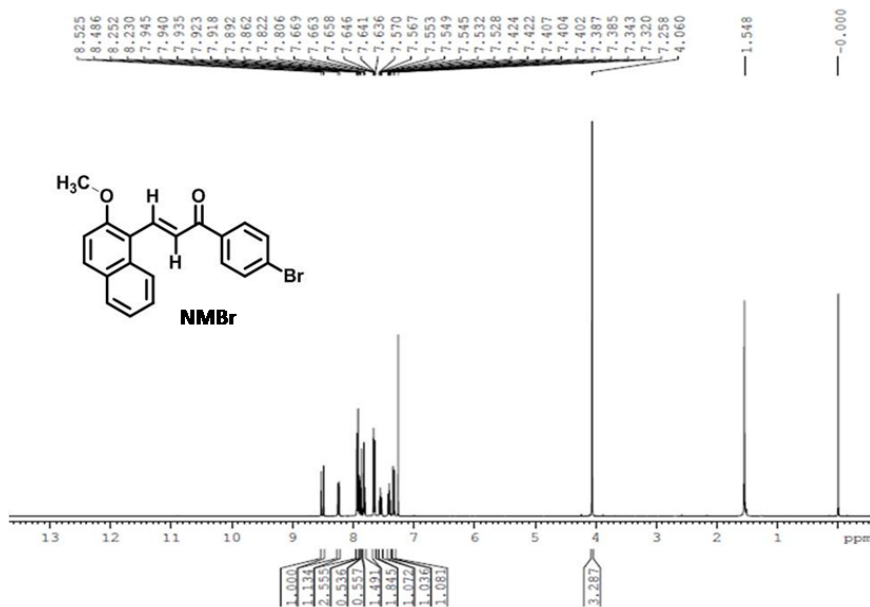
Figure 6.1: ^{1}H NMR spectrum of *(E)-1-(4-bromophenyl)-3-(2-methoxynaphthalen-1-yl)prop-2-en-1-one* (**NMBr).**
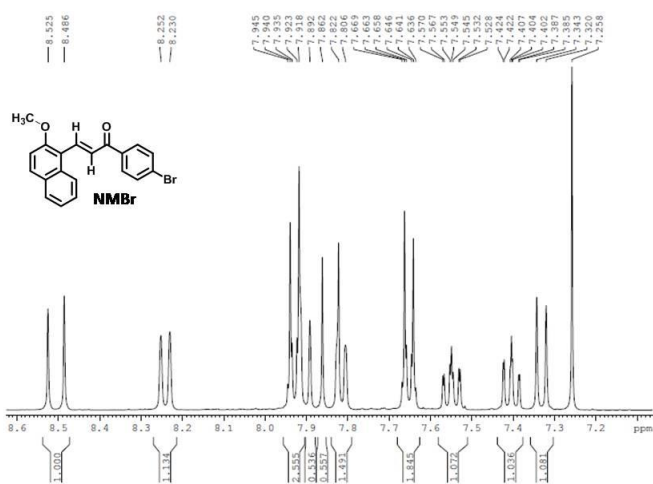
Figure 6.2: ¹H NMR spectrum of *(E)-1-(4-bromophenyl)-3-(2-methoxynaphthalen-1-yl)prop-2-en-1-one* (NMBr) showing region 7.2-8.6 ppm.
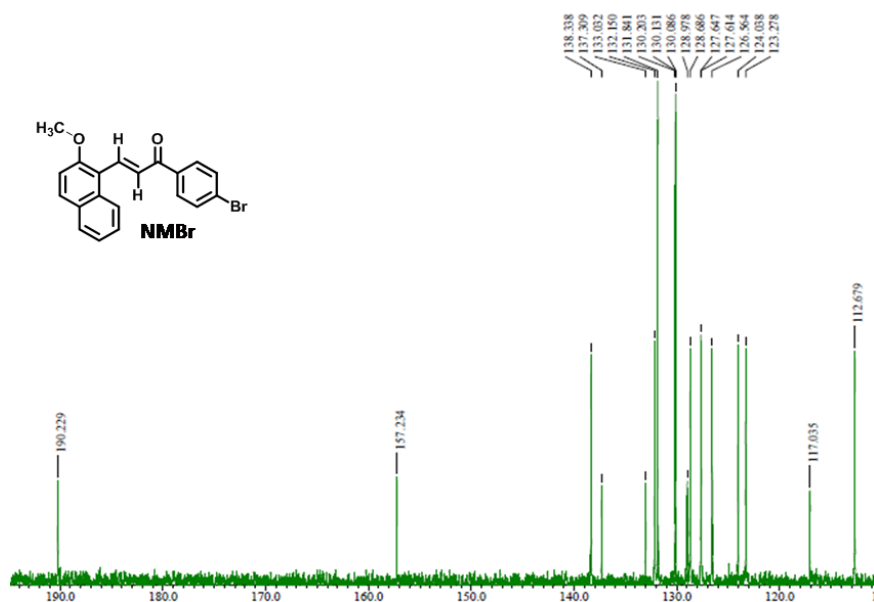
Figure 6.3: ¹³C NMR spectrum of *(E)-1-(4-bromophenyl)-3-(2-methoxynaphthalen-1-yl)prop-2-en-1-one* (NMBr).

(E)-3-(naphthalen-1-yl)-1-phenylprop-2-en-1-one **(PS3): PS3** was synthesized following the method described in Section 6.2.1 from commercially available naphthalene-2-aldehyde (156 mg) and acetophenone (120 mg). Yellow solid. **Yield:** 216 mg (84%). ¹H NMR (800 MHz, CDCl₃): δ 8.08-8.06 (m, 3H), 8.00 (d, J = 16 Hz, 1H), 7.91-7.88 (m, 2H), 7.86 (d, J = 8 Hz, 1H), 7.82 (d, J = 8 Hz, 1H), 7.67 (d, J = 16 Hz, 1H), 7.62 (t, J = 8 Hz, 1H), 7.55-7.53 (m, 4H).

(E)-1-(4-methoxyphenyl)-3-(naphthalen-1-yl)prop-2-en-1-one (**F2OMe**):
F2OMe was synthesized following the method described in Section 6.2.1 from commercially available naphthalene-2-aldehyde (156 mg) and 4-methoxyacetophenone (150 mg). Yellow solid. Yield: 244 mg (85%).^{1}H NMR (400 MHz, CDCl$_3$): δ 8.09 (d, J = 8 Hz, 2H), 7.98 (d, J = 16 Hz, 1H), 7.90-7.80 (m, 5H), 7.68 (d, J = 16 Hz, 1H), 7.53 (d, J = 8 Hz, 2H), 7.01 (d, J = 8 Hz, 2H), 3.91 (s, 3H).

(E)-1-(4-chlorophenyl)-3-(naphthalen-1-yl)prop-2-en-1-one (**F2Cl**): **F2Cl** was synthesized following the method described in Section 6.2.1 from commercially available naphthalene-2-aldehyde (156 mg) and 4-chloroacetophenone (155 mg). Pale yellow solid. Yield: 240 mg (82%). ^{1}H NMR (800 MHz, CDCl$_3$): δ 8.06 (1H), 8.02 (d, J = 8 Hz, 2H), 8.00 (d, J = 16 Hz, 1H), 7.91-7.88 (m, 2H), 7.86 (d, J = 8 Hz, 1H), 7.80 (d, J = 8 Hz, 1H), 7.61 (d, J = 16 Hz, 1H), 7.55 (t, J = 8 Hz, 2H), 7.51 (d, J = 8 Hz, 2H).

(E)-1-(4-bromophenyl)-3-(naphthalen-1-yl)prop-2-en-1-one (**F2Br**): **F2Br** was synthesized following the method described in Section 6.2.1 from commercially available naphthalene-2-aldehyde (156 mg) and 4-bromoacetophenone (199 mg). Pale yellow solid. Yield: 293 mg (87%). ^{1}H NMR (800 MHz, CDCl$_3$): δ 8.06 (1H), 8.00 (d, J = 16 Hz, 1H), 7.94 (d, J = 8 Hz, 2H), 7.91-7.89 (m, 2H), 7.86 (d, J = 8 Hz, 1H), 7.80 (d, J = 8 Hz, 1H), 7.67 (d, J = 8 Hz, 2H), 7.60 (d, J = 16 Hz, 1H), 7.55 (t, J = 8 Hz, 2H).

(E)-3-(2-methoxynaphthalen-1-yl)-1-phenylprop-2-en-1-one (**NMH**): **NMH** was synthesized following the method described in Section 6.2.1 from 2-methoxy-1-naphthaldehyde (**24**) (186 mg) and acetophenone (120 mg). Yellow solid. Yield: 244 mg (85%). ^{1}H NMR (400 MHz, CDCl$_3$): δ 8.49 (d, J = 16 Hz, 1H), 8.25 (d, J = 8 Hz, 1H), 8.06 (d, J = 8 Hz, 2H), 7.88 (d, J = 16 Hz, 1H), 7.89 (d, J = 8 Hz, 1H), 7.81 (d, J = 8 Hz, 1H), 7.57-7.51 (m, 4H), 7.38 (t, J = 8 Hz, 1H), 7.32 (d, J = 8 Hz, 1H), 4.05 (s, 3H).

(E)-3-(2-methoxynaphthalen-1-yl)-1-(4-methoxyphenyl)prop-2-en-1-one

(NM2): NM2 was synthesized following the method described in Section 6.2.1 from 2-methoxy-1-naphthaldehyde **(24)** (186 mg) and 4-methoxyacetophenone (150 mg). Yellow solid, *cis* and *trans* both isomers were obtained. Yield: 228 mg (72%). ^{1}H NMR (400 MHz, CDCl$_3$): δ 8.88 (d, J = 8 Hz,1H), 8.46 (d, J = 16 Hz, 1H), 8.27 (d, J = 8 Hz, 1H), 8.08 (d, J = 8 Hz, 1H), 7.81 (d, J = 8 Hz, 1H), 7.88 (d, J = 16 Hz, 1H), 7.88 (d, J = 8 Hz, 1H), 7.39 (t, J = 8 Hz, 1H)**,** 7.46-7.55 (m, 2H), 7.00 (d, J = 8 Hz, 1H), 6.90 (d, J = 8 Hz, 1H), 4.06 (s, 3H), 3.90 (s, 3H).

(E)-1-(4-chlorophenyl)-3-(2-methoxynaphthalen-1-yl)prop-2-en-1-one **(NMCl):** **NMCl** was synthesized following the method described in Section 6.2.1 from 2-methoxy-1-naphthaldehyde **(24)** (186 mg) and 4-chloroacetophenone (155 mg). Yellow solid. Yield: 268 mg (83%). ^{1}H NMR (400 MHz, CDCl$_3$): δ 8.50 (d, J = 16 Hz, 1H), 8.24 (d, J = 8 Hz, 1H), 7.89-7.94 (m, 3H), 7.84 (d, J = 16 Hz, 1H), 7.81 (d, J = 8 Hz, 2H), 7.65 (t, J = 8 Hz, 2H), 7.40 (t, J = 8 Hz, 1 H), 7.33 (d, J = 8 Hz, 1H), 4.06 (s, 3H). ^{13}C NMR (CDCl$_3$) δ 190.23, 157.24, 138.35, 132.12, 131.86, 130.14, 128.69, 127.65, 126.69, 124.06,123.32, 112.76, 56.36.

(E)-1-(4-bromophenyl)-3-(2-methoxynaphthalen-1-yl)prop-2-en-1-one **(NMBr):** **NMBr** was synthesized following the method described in Section 6.2.1 from 2-methoxy-1-naphthaldehyde **(24)** (186 mg) and 4-bromoacetophenone (199 mg). Yellow solid. Yield: 300 mg (82%). ^{1}H NMR (400 MHz, CDCl$_3$): δ 8.50 (d, J = 16 Hz, 1H), 8.24 (d, J = 8 Hz, 1H), 7.89-7.94 (m, 3H), 7.84 (d, J = 16 Hz, 1H), 7.81 (d, J = 8 Hz, 2H), 7.65 (d, J = 8 Hz, 2H), 7.55 (t, J = 8 Hz, 1H), 7.40 (t, J = 8 Hz, 1H), 7.33 (d, J = 8 Hz, 1H), 4.06 (s, 3H). ^{13}C NMR (CDCl$_3$) δ 190.22, 157.23, 138.38, 131.84, 130.1, 128.9, 127.64, 126.56, 124.03, 123.27, 117.03, 112.67, 56.32.

(E)-1-(4-chlorophenyl)-3-(4-methoxynaphthalen-1-yl)prop-2-en-1-one

(NM1Cl): NM1Cl was synthesized following the method described in Section 6.2.1 from 1-methoxy-4-naphthaldehyde **(27)** (186 mg) and 4-chloroacetophenone (155 mg). Yellow solid. Yield: 203 mg (63%). ^{1}H NMR (400 MHz, CDCl$_3$): δ 8.50

(d, J = 16 Hz, 1H), 8.24 (d, J = 8 Hz, 1H), 8.00 (d, J = 8 Hz, 2H), 7.88 (d, J = 16 Hz, 1H), 7.87 (d, J = 8 Hz, 1H), 7.81 (d, J = 8 Hz, 1H), 7.56(t, J = 8 Hz, 1H), 7.48 (d, J = 8 Hz, 2H), 7.39 (t, J = 8 Hz, 1H), 7.32 (d, J = 8 Hz, 1H), 4.05 (s, 3H).

*(E)-1-(4-bromophenyl)-3-(4-methoxynaphthalen-1-yl)prop-2-en-1-one*

(NM1Br):): NM1Br was synthesized following the method described in Section 6.2.1 from 1-methoxy-4-naphthaldehyde **(27)** (186 mg) and 4-bromoacetophenone (199 mg). Yellow solid. Yield: 245 mg (67%). ^{1}H NMR (800 MHz, CDCl$_3$): δ 8.52 (d, J = 16 Hz, 1H), 8.25 (d, J = 8 Hz, 1H), 7.94 (d, J = 8 Hz, 2H), 7.91 (d, J = 8 Hz, 1H), 7.85 (d, J = 16 Hz, 2H), 7.82 (d, J = 8 Hz, 1H), 7.66 (d, J = 8 Hz, 2H), 7.56 (t, J = 8 Hz, 1H), 7.42 (t, J = 8 Hz, 1H), 7.34 (d, J = 8 Hz, 1H), 4.07 (s, 3H).

(E)-3-(4-methoxynaphthalen-1-yl)-1-(4-nitrophenyl)prop-2-en-1-one

(**NM1NO$_2$**): **NM1NO$_2$** was synthesized following the method described in Section 6.2.1 from 1-methoxy-4-naphthaldehyde **(27)** (186 mg) and 4-nitroacetophenone (165 mg). Yellow solid. Yield: 221 mg (63%). ^{1}H NMR (800 MHz, CDCl$_3$): δ 8.59 (d, J = 16 Hz, 1H), 8.37 (d, J = 8 Hz, 2H), 8.24 (d, J = 8 Hz, 1H), 8.19 (d, J = 8 Hz, 2H), 7.94 (d, J = 8 Hz, 1H), 7.91 (d, J = 16 Hz, 1H), 7.84(d, J = 8 Hz, 1H), 7.58 (t, J = 8 Hz, 1H), 7.43 (d, J = 8 Hz, 1H), 7.35 (d, J = 8 Hz, 1H), 4.10 (s, 3H).

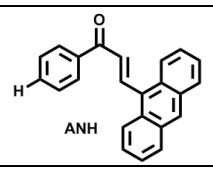## 6.4 Synthetic method for anthracene core chalcone derivative:
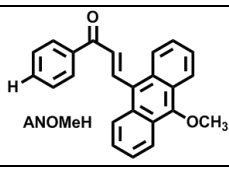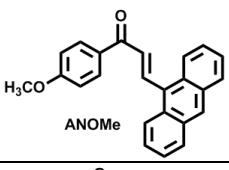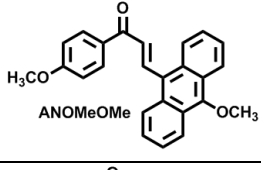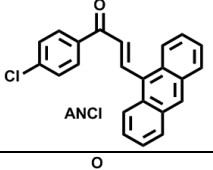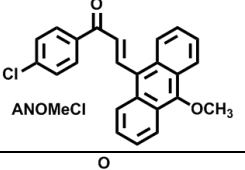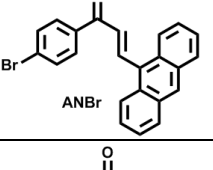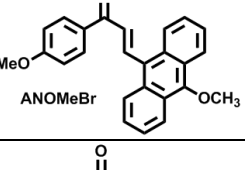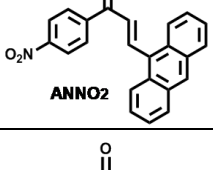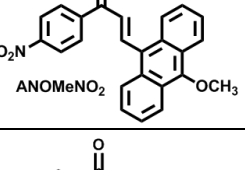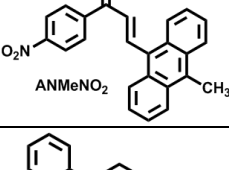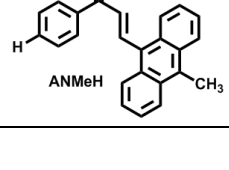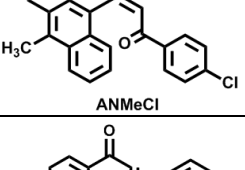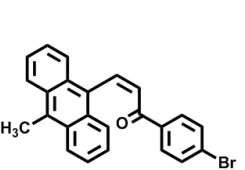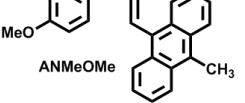
E/Z-3-(9-substitutedanthracen-10-yl)-1-(4-substitutedphenyl) prop-2-en-1-one derivatives have been synthesized by Claisen-Schmidt condensation as shown in (Scheme 6.2). **17** was prepared by the Wittig reaction, one step alkene-forming reaction, on **16** in reasonable yield by reported method [8]. Methylation of **19** with Dimethyl sulfate, using phase transfer catalyst furnished **20**. **18** and **21** were prepared by Vilsmeier Haack reaction on **17** and **20** respectively in modest yields [7]. The physical data of anthracene core chalcone derivatives are tabulated in Table 6.2.
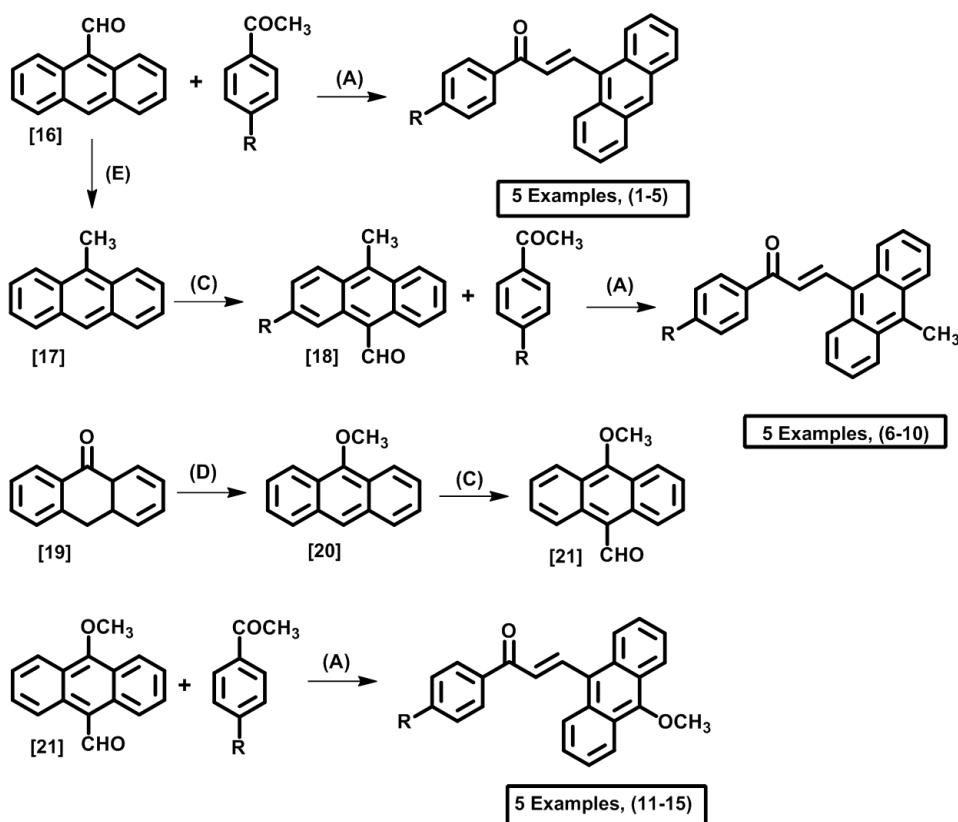
Scheme 6.2: Synthesis of anthracene core chalcone derivatives.

Reagents and conditions: **(A)** 50% NaOH (w/v) in methanol, 60 °C; **(C)** DMF, $C_6H_4Cl_2$, $POCl_3$, 100-110 °C, **(18)** 52%, **(21)** 60%; **(D)** $(CH_3)_2SO_4$, aq.NaOH, CH_2Cl_2, $C_{13}H_{22}ClN$, R.T, 85%; **(E)** $HOCH_2CH_2OCH_2CH_2OCH_2CH_2OH$, NH_2NH_2, aq. KOH, 200°C, 80%.

Table 6.2: Physical data of anthracene core chalcone derivatives.

Compound and code	M.P. (℃)	Compound and code	M.P. (℃)
ANH	120-122	ANOMeH	120-122
ANOMe	114-116	ANOMeOMe	
ANCl	132-134	ANOMeCl	138-140
ANBr	149-151	ANOMeBr	155-157
ANNO2	142-144	ANOMeNO$_2$	195-197
ANMeNO$_2$	172-174	ANMeH	125-127
ANMeCl	139-141	ANMeBr	190-192
ANMeOMe	159-161		

6.5 Characterisation of anthracene core chalcone derivatives:

^{1}H NMR (400 MHz) spectrum of **ANOMeBr** in CDCl₃ solvent is shown in Fig. 6.4, Fig. 6.4a the structure and Fig. 6.5 displays the region δ 7.2-8.6 ppm. A singlet at δ = 4.19 ppm is observed for three H^c protons of the methoxy group. A doublet with J = 16 Hz, centered at δ = 8.81 ppm is observed for H^a proton, another doublet with J = 16 Hz, centered at 7.51 ppm is observed for H^b proton. This confirms the *trans* configuration of the compound. Fig. 6.6 contains the ^{13}C NMR (CDCl₃) spectrum of **ANOMeBr**. δ = 188.56 ppm for the carbonyl carbon, δ = 153.78 ppm appeared for the carbon on the anthracene ring attached to the methoxy group. **ANOMeBr** is taken as a representative compound from the series of anthracene core chalcone derivatives. The other spectral data are tabulated below and spectra are available in the Section 6.12.
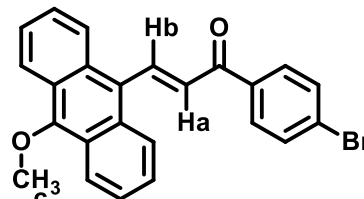
Figure 6.4a: Structure of ANOMeBr.
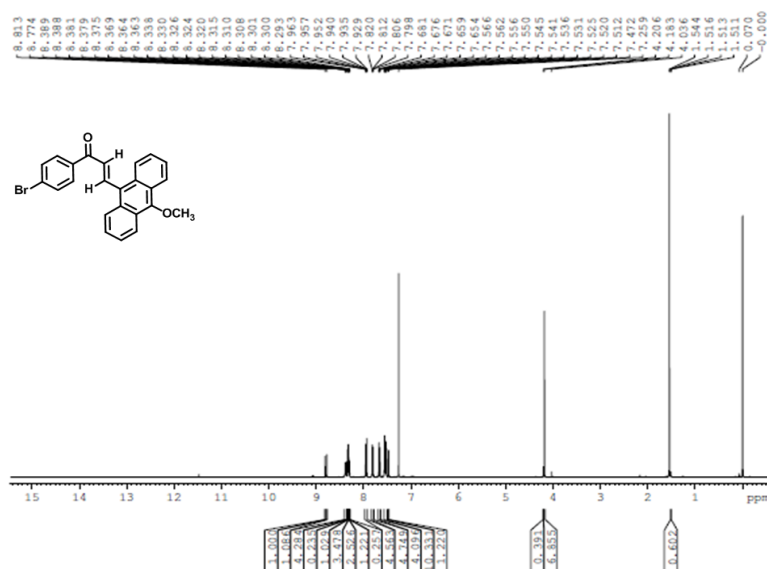
Figure 6.4: ^{1}H NMR spectrum of ANOMeBr.
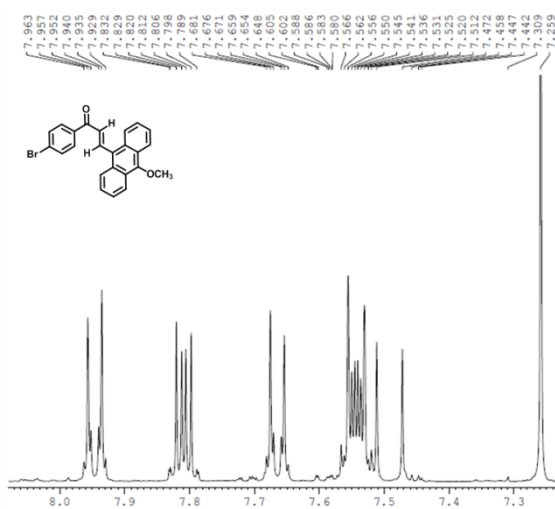
Figure 6.5: ^{1}H NMR spectrum of ANOMeBr in the region 7.2-8.6 ppm.
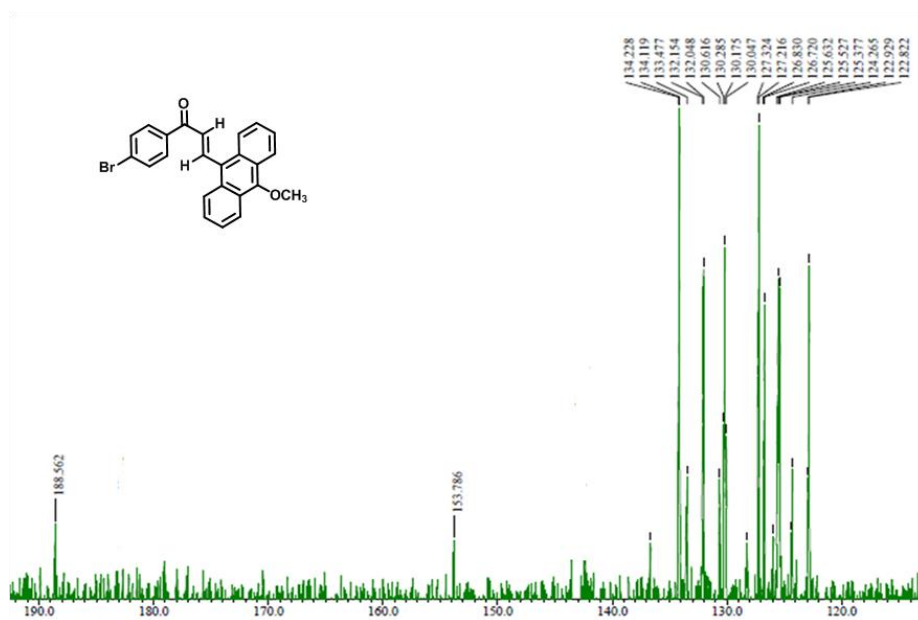
Figure 6.6: ^{13}C NMR spectrum of ANOMeBr.

(E)-3-(anthracen-10-yl)-1-(4-chlorophenyl)prop-2-en-1-one (**ANCl**): A solution of 50% NaOH (w/v) was added to a mixture of 4-chloroacetophenone (1 mmol, 155 mg) and commercially available 9-anthracenecarboxaldehyde (1 mmol, 206 mg) (**16**) in 75 ml of methanol. The mixture was refluxed with continuous stirring for 6 h and then refrigerated overnight. The reaction mixture was neutralized with concentrated HCl, precipitate obtained was collected by filtration and purified by

column chromatography on silica gel (60-120 mesh) using (EtOAc: Hexane = 25: 1) as the eluent. Yield: 272 mg (70%). IR (KBr, cm^{-1}): 3048 (Ar-CH), 1655 (C=O). ^{1}H NMR (400 MHz, CDCl$_3$): δ 8.84 (d, J = 16 Hz, 1H), 8.51 (s, 1H), 8.30 (d, J = 8 Hz, 2H), 8.07-8.03 (m, 4H), 7.94 (d, J = 16 Hz, 1H), 7.56-7.50 (m, 5H), 7.44 (d, J = 8 Hz, 1H).

(E)-3-(anthracen-10-yl)-1-(4-bromophenyl)prop-2-en-1-one (**ANBr**): **ANBr** was synthesized from **16** (1 mmol, 206 mg) and 4-bromoacetophenone (1 mmol, 199 mg) by the same procedure as described for **ANCl** except that the reaction time was 7 h. The product was purified by column chromatography on silica gel (60-120 mesh) using (EtOAc: Hexane=25: 1) as the eluent. Yield: 309 mg (80%). IR (KBr, cm^{-1}): 3046 (Ar-CH), 1662 (C=O). ^{1}H NMR (400 MHz, CDCl$_3$): δ 8.83 (d, J = 16 Hz, 1H), 8.50 (s, 1H), 8.30 (d, J = 8 Hz, 2H), 8.05 (d, J = 8 Hz, 2H), 7.96 (d, J = 8 Hz, 2H), 7.67 (d, J = 8 Hz, 2H), 7.58-7.52 (m, 5H).

(E)-3-(anthracen-10-yl)-1-(4-nitrophenyl)prop-2-en-1-one (**ANNO$_2$**). **ANNO$_2$** was synthesized from **16** (1 mmol, 206 mg) and 4-nitroacetophenone (1 mmol, 165 mg) by the same procedure as described for **ANCl** except that the reaction time was 2 h. The product was purified by column chromatography on silica gel (60-120 mesh) using (EtOAc: Hexane=25: 1) as the eluent. Yield: 307 mg (87%). IR (KBr, cm^{-1})): 3041 (Ar-CH), 1657 (C=O). ^{1}H NMR (400 MHz, CDCl$_3$): δ 8.90 (d, J = 16 Hz, 1H), 8.53 (s, 1H), 8.38 (d, J = 8 Hz, 2H), 8.29 (d, J = 8 Hz, 2H), 8.23 (d, J = 8 Hz, 2H), 8.07 (d, J = 8 Hz, 2H), 7.58 (m, 5H).

(E)-3-(anthracen-10-yl)-1-(4-methoxyphenyl)prop-2-en-1-one (**ANOMe**). **ANOMe** was synthesized from **16** (1 mmol, 206 mg) and 4-methoxyacetophenone (1 mmol, 150 mg) by the same procedure as described for **ANCl** except that the reaction time was 3 h. The product was purified by column chromatography on silica gel (60-120 mesh) using (EtOAc: Hexane=25: 1) as the eluent. Yield: 262 mg (78%). ^{1}H NMR (400 MHz, CDCl$_3$): δ 8.79 (d, J = 16 Hz, 1H), 8.47 (s, 1H), 8.33 (d, J = 8 Hz, 2H), 8.10 (d, J = 8 Hz, 2H), 8.04 (d, J = 8 Hz, 2H), 7.57 (d, J = 16 Hz, 1H), 7.53-7.51 (m, 4H), 7.00 (d, J = 8 Hz, 2H), 3.89 (s, 3H).

(E)-3-(anthracen-10-yl)-1-phenylprop-2-en-1-one (**ANH**). **ANH** was synthesized from **16** (1 mmol, 206 mg) and acetophenone (1 mmol, 120 mg) by the same procedure as described for **ANCl** except that the reaction time was 4 h. The product was purified by column chromatography on silica gel (60-120 mesh) using (EtOAc: Hexane = 25: 1) as the eluent. Yield: 206 mg (67%). IR (KBr, cm^{-1}): 3049 (Ar-CH), 1655 (C=O). ^{1}H NMR (400 MHz, CDCl$_3$): δ 8.82 (d, J = 16 Hz, 1H), 8.48 (s, 1H), 8.33 (d, J = 8 Hz, 2H), 8.11 (d, J = 8 Hz, 2H), 8.05 (d, J = 8 Hz, 2H), 7.59 (d, J = 16 Hz, 2H), 7.54-7.52 (m, 5H). 7.62 (d, J = 8 Hz, 1H).

(E)-1-(4-chlorophenyl)-3-(9-methylanthracen-10-yl)prop-2-en-1-one

(**ANMeCl**). 9-methylanthracene-10-carbaldehyde (**18**) was synthesized from commercially available **16** in aqueous KOH solution and hydrazine hydrate following the reported procedure [9].

A 50% NaOH (w/v) solution was added to a mixture of 4-chloroacetophenone (1 mmol, 155 mg) and (**18**) (1 mmol, 220 mg) in 25 ml of methanol. The mixture was refluxed with continuous stirring for 6 h and then refrigerated overnight. The reaction mixture was neutralized with concentrated HCl and precipitate obtained was collected by filtration and purified using column chromatography on silica gel (60-120 mesh) using (EtOAc: Hexane=1: 20), *trans* 20%. Yield: 192 mg (54%). IR (KBr, cm^{-1}): 3032 (Ar-CH), 1674 (C=O). ^{1}H NMR (400 MHz, CDCl$_3$): δ 8.38 (d, J = 12 Hz, 1H), 8.35-8.31 (M, 4 H), 8.04 (d, J = 8 Hz, 2H), 7.82 (d, J = 8 Hz, 2H), 7.57 (d, J = 8 Hz, 2H), **7.52** (d, J = 8 Hz, 2H), 7.48 (d, J = 12 Hz, 1H), 3.17 (s, 3H).

(Z)-1-(4-bromophenyl)-3-(9-methylanthracen-10-yl)prop-2-en-1-one

(**ANMeBr**). **ANMeBr** was synthesized from **18** (1 mmol, 220 mg) and 4-bromoacetophenone (1 mmol, 199 mg) by the same procedure as described for **ANMeCl**. The product was purified by column chromatography on silica gel (60-120 mesh) using (EtOAc: Hexane=1: 20) as the eluent. Yield: 236 mg (59%). IR (KBr, cm^{-1}): 3026 (Ar-CH), 1666 (C=O). ^{1}H NMR (400 MHz, CDCl$_3$): δ 8.26 (d, J = 8 Hz, 2H), 8.09 (d, J = 8 Hz, 2H), 8.00 (d, J = 8 Hz, 1H), 7.51-7.44 (m, 5H), 7.29 (d, J = 8 Hz, 2H), 7.08 (d, J = 8 Hz, 2H), 3.06 (s, 3H).

(E)-3-(9-methylanthracen-10-yl)-1-(4-nitrophenyl)prop-2-en-1-one

(ANMeNO₂). **ANMeNO₂** was synthesized from **18** (1 mmol, 220 mg) and 4-nitroacetophenone (1 mmol, 165 mg) by the same procedure as described for **ANMeCl** except that the reaction time was 1 h. The product was purified by column chromatography on silica gel (60-120 mesh) using (EtOAc: Hexane=1: 10) as the eluent. Yield: 300 mg. (78%). IR (KBr, cm^{-1}): 3031(Ar-CH), 1658 (C=O). ^{1}H NMR (400 MHz, CDCl$_3$): δ 8.91 (d, J = 16 Hz, 1H), 8.39-8.36 (m, 4H), 8.32 (d, J =8 Hz, 2H), 8.22 (d, J = 8 Hz, 2H), 7.54-7.60 (m, 4H), 7.51 (d, J = 16 Hz, 1H), 3.17 (s, 3H).

(E)-3-(9-methylanthracen-10-yl)-1-(4-methoxyphenyl)prop-2-en-1-one

(ANMeOMe). **ANMeOMe** was synthesized from **18** (1 mmol, 220 mg) and 4-methoxyacetophenone (1 mmol, 150 mg) by the same procedure as described for **ANMeCl** except that the reaction was refluxed for 7 h and stirred at rt for 5 h. The product was purified by column chromatography on silica gel (60-120 mesh) using (EtOAc: Hexane=40: 1) as the eluent. *trans* 75%. Yield: mg. (67%). ^{1}H NMR (400 MHz, CDCl$_3$): δ 8.80 (d, J = 16 Hz, 1H), 8.36 (t, J = 8 Hz, 2H), 8.10 (d, J = 8 Hz, 2H), 7.57-7.50 (m, 5H), 7.00 (d, J = 8 Hz, 2H), 3.90 (s, 3H), 3.17 (s, 3H).

(Z)-3-(9-methylanthracen-10-yl)-1-phenylprop-2-en-1-one **(ANMeH)**. **ANMeH** was synthesized from **18** (1 mmol, 220 mg) and acetophenone (1 mmol, 120 mg) by the same procedure as described for **ANMeCl** except that the reaction time was 4 h. The product was purified by column chromatography on silica gel (60-120 mesh) using (EtOAc: Hexane=1: 10) as the eluent. Yield: 58%. IR (KBr, cm^{-1}): 2932 (Ar-CH), 1660 (C=O). ^{1}H NMR (400 MHz, CDCl$_3$): δ 8.36 (d, J = 8 Hz, 2H), 8.26 (d, J = 8 Hz, 2H), 8.14 (d, J = 8 Hz, 2H), 8.11 (d, J = 8 Hz, 2H), 7.93 (d, J = 12 Hz, 1H), 7.48 (d, J = 8 Hz, 2H), 7.45 (d, J = 12 Hz, 1H), 7.52-7.56 (m, 3H)**,** 3.05 (s, 3H). E: Z= 47: 53.

(E)-1-(4-chlorophenyl)-3-(9-methoxyanthracen-10-yl)prop-2-en-1-one

(ANOMeCl). 10-methoxy 9-anthraldehyde **(21)** was prepared according to the known procedure. Anthrone **(19)** on methylation with dimethyl sulphate provides

9-methoxyanthracene **(20)**. **20** On Vilsmeier reaction with dimethyl formamide and phosphorus oxychloride yields **21** [8]**.**

A 50% NaOH (w/v) solution was added to a mixture of 4-chloroacetophenone (1 mmol, 155 mg) and **(21)** (1 mmol, 236 mg) in 125 ml of methanol. The mixture was refluxed with continuous stirring for 3 h and then refrigerated overnight. The reaction mixture was neutralized with concentrated HCl and precipitate obtained was collected by filtration and purified using column chromatography on silica gel (60-120 mesh) using (EtOAc: Hexane=1: 4), Yield: 193 mg (52%). IR (KBr, cm^{-1}): 3056 (Ar-CH), 1657 (C=O). ^{1}H NMR (400 MHz, CDCl$_3$): δ 8.80 (d, J = 16 Hz, 1H), 8.39 (d, J = 8 Hz, 1H), 8.34-8.32 (m, 4H)**,** 8.03 (d, J = 8 Hz, 1H), 7.83-7.80 (m, 3H)**,** 7.56-7.49 (m, 4H), 4.19 (s, 3H).

(E)-1-(4-bromophenyl)-3-(9-methoxyanthracen-10-yl)prop-2-en-1-one
(ANOMeBr). **ANOMeBr** was synthesized from **21** (1 mmol, 236 mg) and 4-bromoacetophenone (1 mmol, 199 mg) by the same procedure as described for **ANOMeCl** except that the reaction time was 3 h. The product was purified by column chromatography on silica gel (60-120 mesh) using (EtOAc: Hexane = 1: 4) as the eluent. Yield: 308 mg (74%). IR (KBr, cm^{-1}): 3064 (Ar-CH), 1673 (C=O). ^{1}H NMR (400 MHz, CDCl$_3$): δ 8.81 (d, J = 16 Hz, 1H), 8.40-8.37 (m, 1H), 8.33 (m, 4H)**,** 7.96 (d, J = 8 Hz, 2H), 7.82 (d, J = 8 Hz, 2H), 7.67 (d, J = 8 Hz, 1H), 7.57-7.54 (m, 2H), 7.51 (d, J = 16 Hz, 1H), 4.19 (s, 3H).

(E)-3-(9-methoxyanthracen-10-yl)-1-(4-nitrophenyl)prop-2-en-1-one
(ANOMeNO$_2$). **ANOMeNO$_2$** was synthesized from **21** (1 mmol, 236 mg) and 4-nitroacetophenone (1 mmol, 165 mg) by the same procedure as described for **ANOMeCl** except that the reaction time was 2 h. The product was purified by column chromatography on silica gel (60-120 mesh) using (EtOAc: Hexane = 25: 1) as the eluent. Yield: 325 mg (85%). IR (KBr, cm^{-1}): 3071 (Ar-CH), 1664 (C=O). ^{1}H NMR (400 MHz, CDCl$_3$): δ 8.88 (d, J = 16 Hz, 1H), 8.38 (d, J = 8.0 Hz, 2H), 8.34-8.31 (m, 2H), 8.23 (d, J = 12.0 Hz, 2H), 7.54 (d, J = 16 Hz, 1H), 7.58 (d, J = 8 Hz, 4H), 4.20 (s, 3H).

(E)-3-(9-methoxyanthracen-10-yl)-1-(4-methoxyphenyl)prop-2-en-1-one
(ANOMeOMe). **ANOMeOMe** was synthesized from **21** (1 mmol, 236 mg) and 4-methoxyacetophenone (1 mmol, 150 mg) by the same procedure as described for **ANOMeCl** except that the reaction was refluxed for 7 h and stirred at rt for 5 h. The product was purified by column chromatography on silica gel (60-120 mesh) using (EtOAc: Hexane=40: 1) as the eluent. Yield: 257 mg (70%). E: Z=66: 34 ^{1}H NMR (400 MHz, CDCl$_3$): δ 8.77 (d, J = 16 Hz, 1H), 8.36 (t, J = 8 Hz, 4H), 8.10 (d, J = 8 Hz, 2H), 7.57-7.53 (m, 4H)**,** 7.45 (m, 2H), 7.00 (d, J = 8 Hz, 1H), 4.19 (s, 3H), 3.90 (s, 3H)**.**

(E)-3-(9-methoxyanthracen-10-yl)-1-phenylprop-2-en-1-one   **(ANOMeH)**. **ANOMeH** was synthesized from **21** (1 mmol, 236 mg) and acetophenone (1 mmol, 120 mg) by the same procedure as described for **ANOMeCl** except that the reaction time was 7 h. The product was purified by column chromatography on silica gel (60-120 mesh) using (EtOAc: Hexane=1: 4) as the eluent. Yield: 250 mg (74%). IR (KBr, cm^{-1}): 3069 (Ar-CH), 1663 (C=O). ^{1}H NMR (400 MHz, CDCl$_3$): δ 8.80 (d, J = 16 Hz, 1H), 8.40-8.34 (m, 4H), **8.39 (d, J = 8 Hz, 2H),** 8.35 (d, J = 8 Hz, 2H), 8.10 (d, J = 8 Hz, 1H), 7.62 (d, J = 8 Hz, 1H), 7.59-7.53 (m, 5H), 4.19 (s, 3H).

6.6 Linear optical properties of naphthalene fused chalcones:

The spectra were recorded at room temperature in chloroform solution with a concentration of 0.5×10^{-8} M. The experimental photophysical characteristics of the investigated *(E)-1-(4-substitutedphenyl)-3-(naphthalen-1-yl)prop-2-en-1-one derivatives* are summarized in Table 6.3 & Fig. 6.7 shows the absorption spectra.

Table 6.3: Photo Physical data of *(E)-1-(4-substituted phenyl)-3-(naphthalen-1-yl)prop-2-en-1-one* **derivatives.**

Cmpd	λ_{abs} (nm)	λ_{em} (nm)
PS3	327	446(329)
F2OMe	329	441, 533 (329)
F2Cl	281, 330	437 (330)
F2Br	226, 329	399(329)

The chromophores show an intense absorption band in the near UV–blue visible region (Fig. 6.7). Two strong peaks in the UV-region, due to $n - \pi^*$ and $\pi - \pi^*$ transition, is attributable to the presence of aromatic ring and C=O group. The $n - \pi^*$ transition band is observed in the range 327-330 nm, with a change in substituent in the chalcone ring A, no major difference in the absorption band was observed.

The photoluminescence spectra are presented in Fig. 6.8. The emission characteristics depend on the substituent present in the molecule. In **F2OMe** two emission peaks are visible probably due to aggregation formation and in **F2Br**, interestingly; the dual peak nature of the emission spectrum is also observed due to TICT.
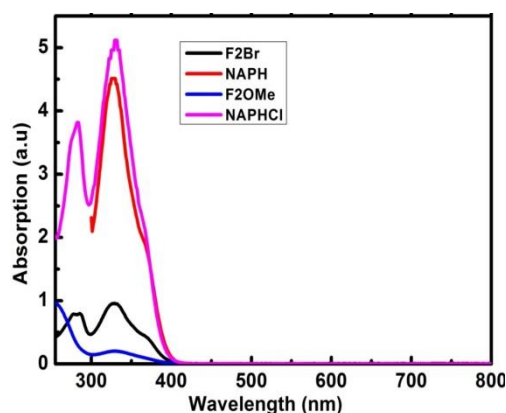
Figure 6.7: Absorption Spectra of *(E)-1-(4-substituted phenyl)-3-(naphthalen-1-yl)prop-2-en-1-one* **derivatives.**
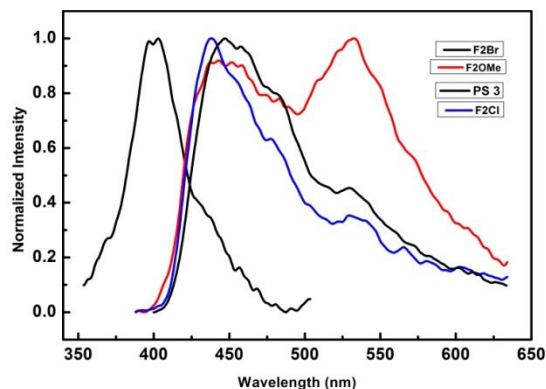
Figure 6.8: Emission spectra of *(E)-1-(4- substituted phenyl)-3-(naphthalen-1-yl)prop-2-en-1-one* **derivatives.**

Absorption maxima and emission maxima of *(E)-1-(4-substitutedphenyl)-3-(2-methoxynaphthalen-1-yl)prop-2-en-1-one* and *(E)-1-(4-substitutedphenyl)-3-(4-methoxynaphthalen-1-yl)prop-2-en-1-one* derivatives are outlined in Table 6.4 in chloroform solution with 0.5×10^{-8} M concentration.

Table 6.4: Photo Physical data of *(E)-1-(4-substitutedphenyl)-3-(2/4-methoxynaphthalen-1-yl)prop-2-en-1-one* **derivatives.**

| Compound	λ_{abs} (nm)	λ_{em} (nm)
NMH	264, 380	409 (379)
NM2	267, 379	395 (379)
NMCl	280, 327	487 (327)
NMBr	270, 386	427, 432 (380)
NM1Cl	268, 385	502, 514 (385)
NM1Br	267, 384	482 (384)

This series of six chalcones can be bifurcated into two set according to the position of the methoxy group in the naphthalene ring. One set consists of four compounds (**NMH, NM2, NMCl, NMBr**) and the other have **NM1Cl, NM1Br.** Absorption maxima ranged from 327-386 nm. Weakly positive groups –Cl and –Br have small or no consequence when present on ring A of chalcone as seen in the case of **NM1Cl, NM1Br** & **NMBr**. The λ max value of the chalcones, substituted on phenyl ring A have less sensitivity compared to that of ring B. If substituents of strongly positive electromeric character (here, –OCH$_3$) are present in both ring, as in the case of **NM2**, the consequential bathochromic effects have the same magnitude as those caused by only one group present on ring B [10, 11]. For e.g. **NMH** and **NM2** have λ_{max} value 380 and 379 nm respectively. The absorption and
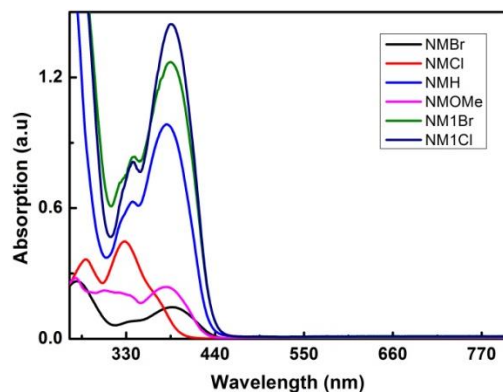
Figure 6.9: Absorption Spectra of naphthalene core chalcone derivatives.
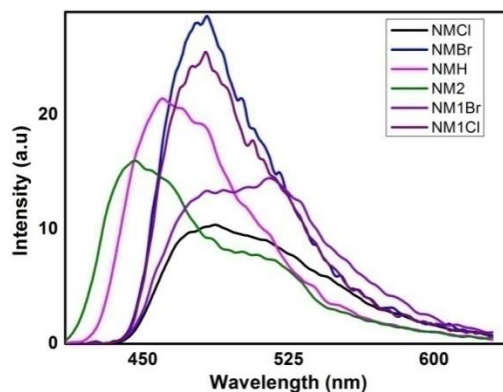
Figure 6.10: Emission Spectra of naphthalene core chalcone derivatives.

emission spectra are presented in Fig. 6.9 and Fig. 6.10 respectively. In the series, highest Stokes shift of 117 nm is observed for **NM1Cl** probably because of stable excited state(s) in a polar solvent like chloroform.

6.7 Nonlinear optical properties of naphthalene fused chalcones.

Up-conversion photoluminescence (UCPL) of naphthalene fused chalcone derivatives were studied in chloroform solution with concentration of 2.0×10^{-3} M and 100 mW laser power.

Up-conversion is the phenomenon where one or more photons of lower energy are absorbed, either simultaneously or sequentially, and re-emitted as a higher energy photon i.e. spectrally blue shifted to the wavelength of the excitation of photons. Up-converters are those compounds able to exhibit this process. Fig. 6.11 schematically explains the UCPL process.

Among many mechanisms, one is two-photon absorption (discussed in Section 1.5). The "virtual state" (denoted by dotted lines in Fig. 6.11) has a very short lifetime; two-photon absorption occurs only if the second photon gets there before the virtual state is decayed. Thus, TPA is a nearly concerted process that demands a high density (flux) of incident photons. Intense laser irradiation can bring about two or multiphoton absorption (2PA, 3PA, etc.), in some known organic dyes consisting anthracene, phenanthrene moieties etc [12, 13]. Commonly used fluorescent dye emits in the visible range after absorbing ultraviolet (UV) radiation. But, in the case of TPA organic molecule, the situation is reversed. It can be tuned to absorb infrared (IR) radiation and generate laser emission in the visible range.
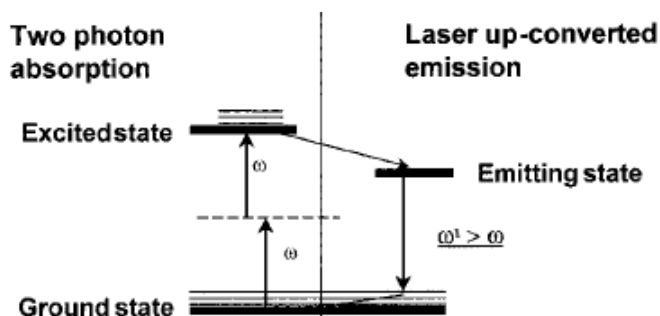
Figure 6.11: Frequency up-converted fluorescence via two photon absorption by simultaneous two photon absorption.

It is interesting that, after excitation by a TPA process, the molecule undergoes one-photon fluorescence emission from the excited state to return to the ground state. The probability of a TPA depends linearly on the square of the incident light intensity (discussed in Section 1.5), So, there is negligible absorption in any out-of-focus volume and photoexcitation is spatially restricted to the focal volume. The detailed information on the quantum mechanical description of the theory of TPA can be found elsewhere [14-19].The UCPL studies on chalcones are discussed below.
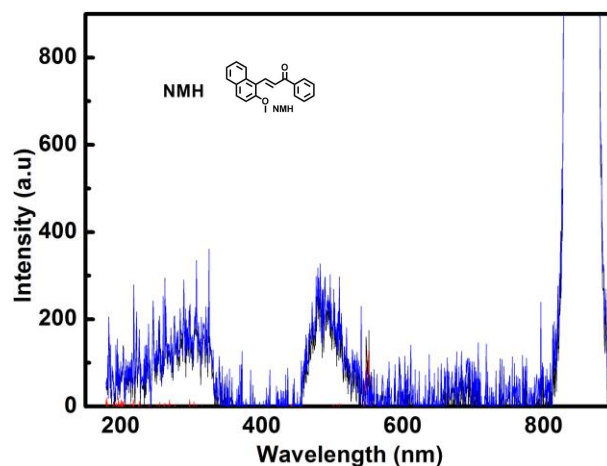
Figure 6.12: UCPL spectrum of NMH at 845 nm excitation.
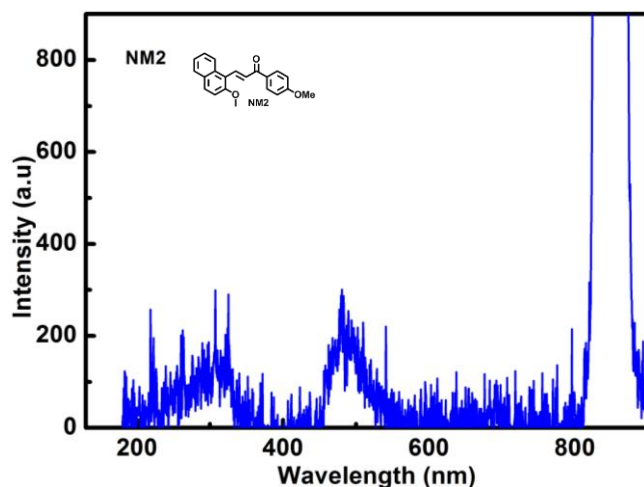
Figure 6.13: UCPL spectrum of NM2 at 845 nm excitation.
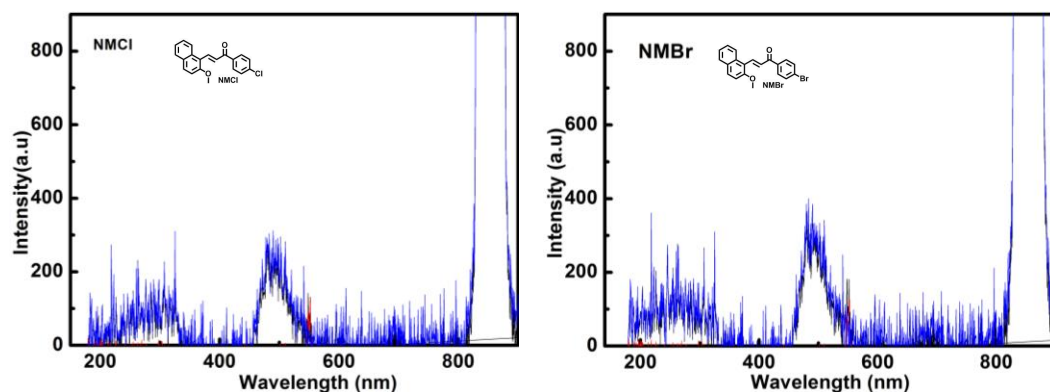
Figure 6.14: UCPL spectrum of NMCl and Figure 6.15: UCPL spectrum of NMBr at 845 nm excitation.

The UCPL spectra of *(E)-1-(4-substitutedphenyl)-3-(2-methoxynaphthalen-1-yl)prop-2-en-1-one* (**NMH, NMCl, NMBr, NM2**) and *(E)-1-(4-substitutedphenyl)-3-(4-methoxynaphthalen-1-yl)prop-2-en-1-one derivatives* (**NM1Cl, NM1Br**) are presented in Fig. 6.12-6.17
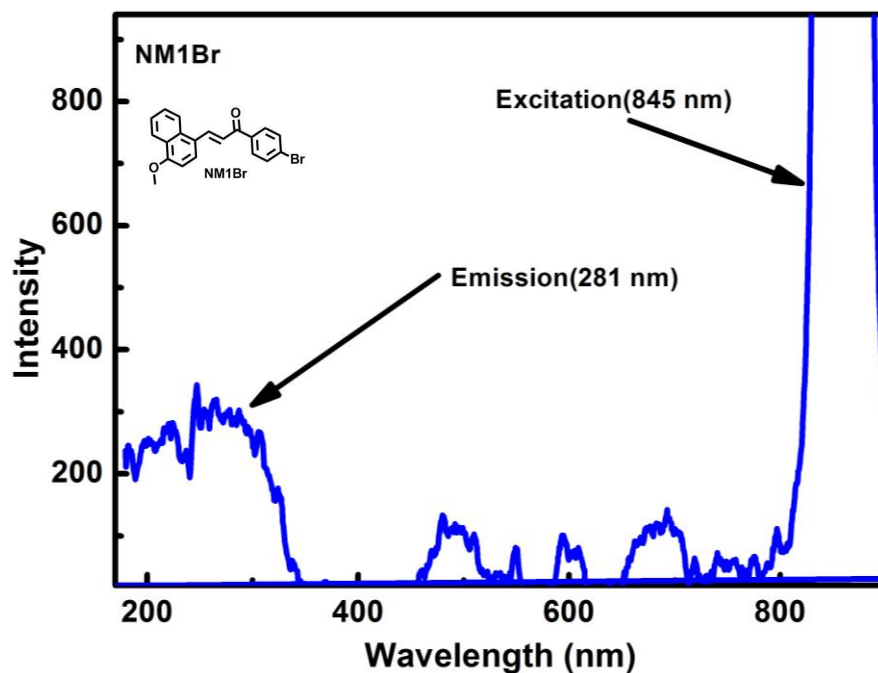
Figure 6.16: UCPL spectrum of NM1Br at 845 nm excitation.

It is very clear from the spectra that the *(E)-1-(4-substitutedphenyl)-3-(2/4-methoxynaphthalen-1-yl)prop-2-en-1-one* compounds absorbs 845 nm light and emits in the UV region (280-285 nm) displaying blue luminescence. It is probable that

due to three-photon absorption up-converted blue luminescence is observed; emission in the range of 400-420 nm is also present probably because of two-photon absorption and corresponding one photon luminescence.

Studies on *(E)-1-(4-substitutedphenyl)-3-(naphthalen-1-yl)prop-2-en-1-one derivatives* (**F2Br, F2Cl, PS 3** and **F2OMe**) were also carried out to examine their up-conversion capacity. But no detectable signal was received, though these compounds also contain naphthalene in their core structure. But when the chalcones have methoxy group in the naphthalene ring, either in position 2 or in position 4, their nonlinear optical properties do changes abruptly. From Fig. 6.17 it is noticeable that **NM1Cl** (Fig. 6.17) has the highest intensity emission in the region in the series.

Figure 6.17: UCPL spectrum of NM1Cl at 845 nm excitation.

6.8 Linear optical properties of anthracenyl chalcone derivatives:

In compounds **1-5** the chalcone derivatives have un-substituted 9-position in the anthracene moiety. For derivatives **6-10** the 9-position in the anthracene moiety is substituted with methyl group followed by methoxy substitution for compounds **11-15** as shown in Scheme 6.2. The photophysical data is assimilated in Table 6.5.

The three types of series, with increasing electron donor strength, have one thing in
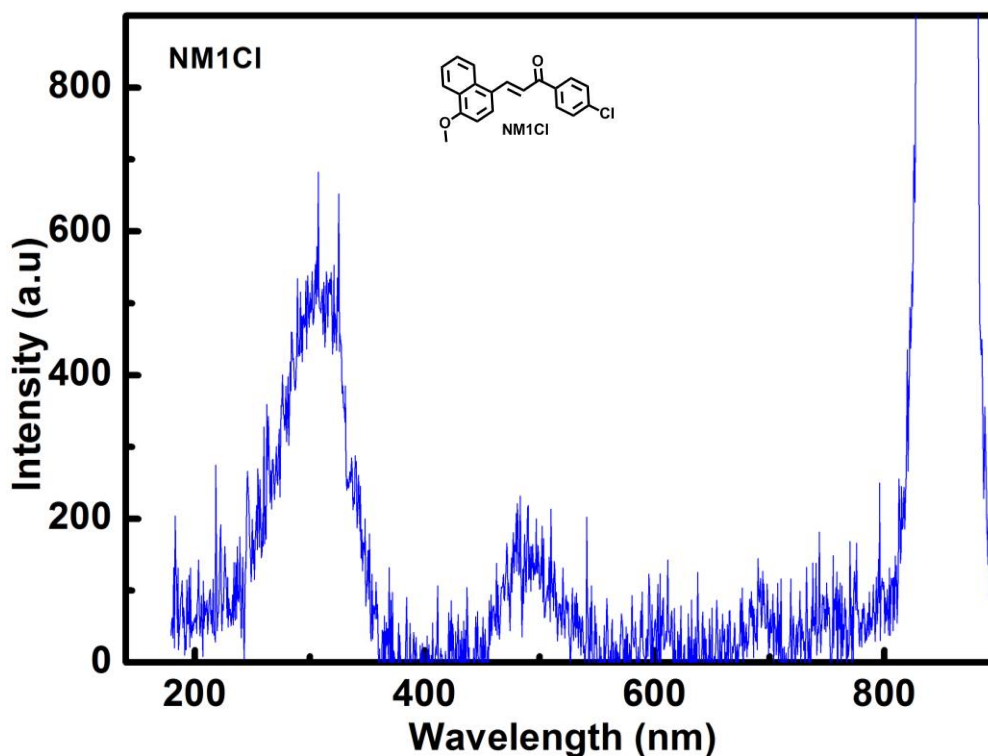
Table 6.5: Photophysical data of anthracenyl chalcone derivatives.

Compound	λ_{abs} (nm)	λ_{em} (nm)	$\Delta\bar{v}$ cm^{-1}	Compound	λ_{abs} (nm)	λ_{em} (nm)	$\Delta\bar{v}$ cm^{-1}
1. (R=a)	415, 258	302 (Ex 258)	5647	6. (R=a)	399, 254	430 (Ex 399)	1806
2. (R=b)	416, 252	532 (Ex 416)	5241	7. (R=b)	392, 262	436 (Ex 392)	2574
3. (R=c)	437, 258	567 (Ex 437)	5246	8. (R=c)	455,260	525 (Ex 455)	2930
4. (R=d)	390,256	523 (Ex 390)	6520	9. (R=d)	399, 303	399 (Ex 258)	5531
5. (R=e)	414	528 (Ex 414)	5215	10. (R=e)	391, 261	531 (Ex 391)	6743
11. (R=a)	327, 250	547 (Ex 327)	1229	13. (R=c)	449, 257	543 (Ex 449)	3855
12. (R=b)	424, 258	535 (Ex 424)	4893	14. (R=d)	432, 258	538 (Ex 432)	4560
15. (R=e)	419, 257	296 (Ex 419)	5126				

common that the nitro derivative of all of them (**ANNO$_2$, ANMeNO$_2$, ANOMeNO$_2$**) shows the highest λ_{abs} value. Fig. 6.18 accumulates the three compounds in the spectra, almost all of them have a transparent window for 520-800 nm and reveals absorption n-π^* and π-π^* transition characteristic of molecules containing a carbonyl group.
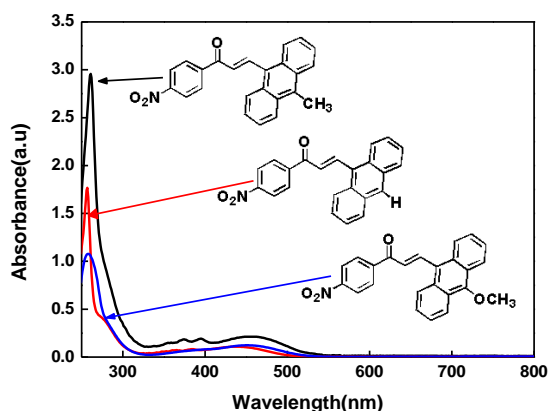
Figure 6.18: Absorption spectra of ANNO$_2$, ANMeNO$_2$ and ANOMeNO$_2$.
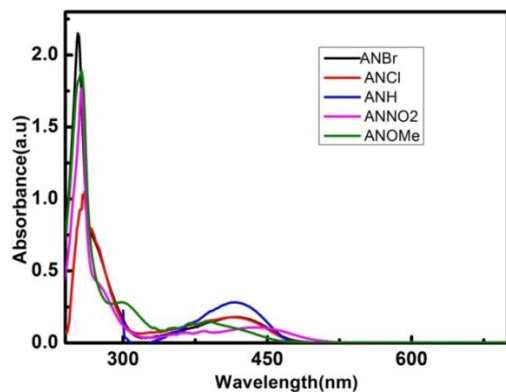
Figure 6.19: Absorption spectra of *(E)/(Z)-3-(anthracen-10-yl)-1-(4-substitutedphenyl)prop-2-en-1-one* compounds.

Figure 6.20: Absorption spectra of *(E)-1-(4-substitutedphenyl)-3-(9-methoxyanthracen-10-yl)prop-2-en-1-one* compounds.

The absorption spectra of five (**ANBr, ANCl, ANH, ANNO$_2$, ANOMe**) *(E)/(Z)-3-(anthracen-10-yl)-1-(4-substitutedphenyl)prop-2-en-1-one* derivatives in chloroform with a dilute solution, are shown in Fig. 6.19 and **t**he absorption spectra of five *(E) 1-(4-substitutedphenyl)-3-(9-methoxyanthracen-10-yl)prop-2-en-1-one* derivatives namely (**ANOMeBr, ANOMeCl, ANOMeH, ANOMeNO$_2$** and **ANOMeOMe**) are presented in Fig. 6.20, absorption spectra of *(E) 1-(4-substitutedphenyl)-3-(9-methylanthracen-10-yl)prop-2-en-1-one* derivatives namely (**ANMeBr, ANMeCl, ANMeH, ANMeNO$_2$** and **ANMeOMe**) in Fig. 6.21.

The ultraviolet spectrum of the polynuclear aromatic hydrocarbons possesses characteristic shapes and fine structure. If the spectra of substituted anthracene derivatives (Fig. 6.21), is compared on the basis of similarity of peaks and the fine
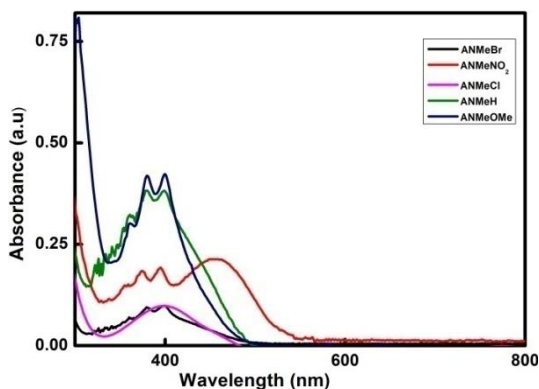
Figure 6.21: The absorption spectra of ANMeBr, ANMeCl, ANMeH, ANMeNO$_2$ and ANMeOMe.

structure, with the spectra of the un-substituted one (Fig. 6.19), the nature of the chromophore can be clearly identified of 9-methyl anthracene [20].

The emission spectra of *(E)/(Z)-3-(anthracen-10-yl)-1-(4-substitutedphenyl)prop-2-en-1-one*, *(E)-1-(4-substitutedphenyl)-3-(9-methoxyanthracen-10-yl)prop-2-en-1-one* and *(E)-1-(4-substitutedphenyl)-3-(9-methylanthracen-10-yl)prop-2-en-1-one* are presented in Fig. 6.22, 6.23 and 6.24 respectively.

The fluorescence spectra were recorded by exciting with the compounds with their corresponding absorption maxima in chloroform solution. The compounds exhibited high Stokes shifts, ranging from 1229 to 6743 cm^{-1} (see Table 6.5). Stokes shift is a physical constant of luminescent molecules and it indicates the energy dissipated in bringing about ionization during the lifetime of excited state before
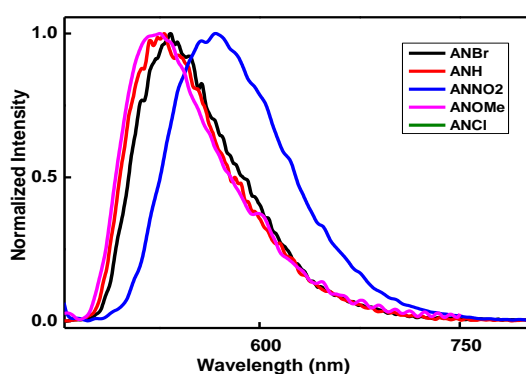
Figure 6.22: Emission spectra of *(E)/(Z)-3-(anthracen-10-yl)-1-(4-substitutedphenyl)prop-2-en-1-one* compounds when excited at their absorption maxima.
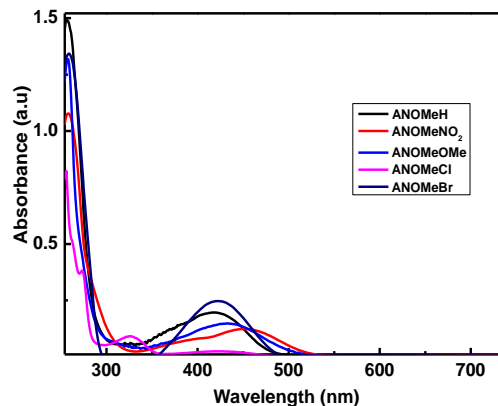
Figure 6.23: Emission spectra of *(E)-1-(4-substitutedphenyl)-3-(9-methoxyanthracen-10-yl)prop-2-en-1-one* compounds when excited at their absorption maxima.

Figure 6.24: Emission spectra of (E)-1-(4-substitutedphenyl)-3-(9-methylanthracen-10-yl)prop-2-en-1-one compounds when excited at their absorption maxima.

return to the ground state. The magnitude of the shift depends on factors such as solvent polarity, viscosity, and polarizability. It also depends on whether the excited state can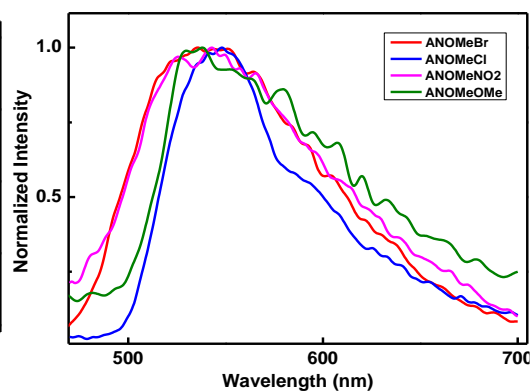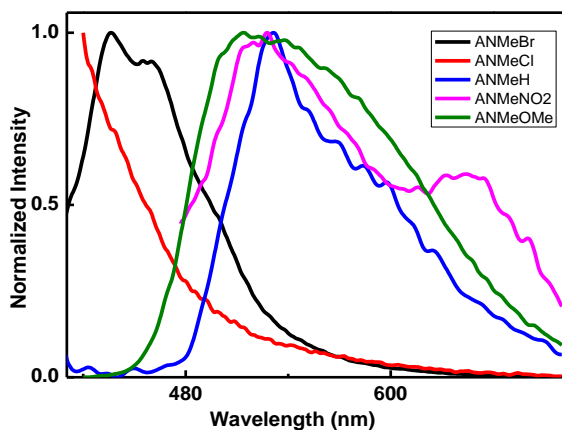 undergo any specific interactions such as proton transfer or charge transfer to other molecules or (sometimes) within the same molecule. Large Stokes shift for most of the compounds indicates that the environment is not rigid so rearrangement is possible. Now, these fluorophores can be utilized in many ways, including, labels for biomolecules, enzyme substrates, environmental indicators, and cellular stains. But, fluorophores with small Stokes shifts are vulnerable to self-quenching *via* energy transfer; therefore the number of labels that can be attached to a biomolecule gets reduced. Stokes shifts of greater than 80 nm are desirable to minimize reabsorption of emitted photons [21, 22]. TICT (Twisted intramolecular charge transfer) is reflected in the emission spectra having dual peak nature in **ANOMeBr, ANMeBr** and **ANNO$_2$**. Again, **ANMeNO$_2$** also indicates the formation of aggregation through two emission peak (525 nm and 644 nm). The emission band at 644 nm with reduced intensity and red shifted is likely due to the formation of H-aggregates formed through parallel stacking of molecules with a "face-to-face" orientation in this medium.

6.9 Nonlinear optical properties of anthracene core chalcones:
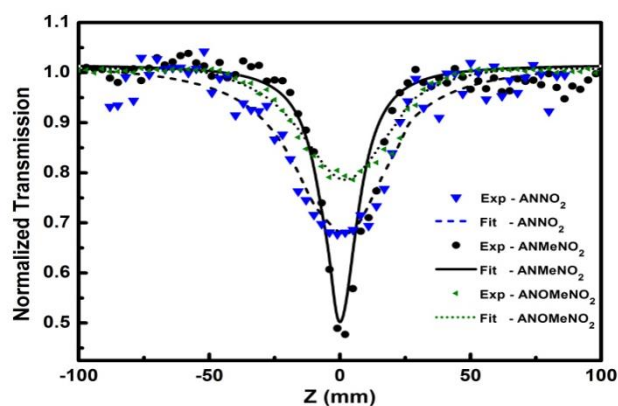
Figure 6.25: Open aperture z-scan data of ANNO$_2$, ANMeNO$_2$ and ANOMeNO$_2$

The open aperture z-scan experimental data of the anthracene core chalcone was fitted to Eqn. 4.3 and Fig. 6.25 shows the fitted z-scan data of the three nitro derivatives (**ANNO$_2$, ANMeNO$_2$, ANOMeNO$_2$**) in 1.3×10^{-8} M chloroform solution. The corresponding fitted values for other compounds of this series are incorporated in Fig. 6.27; the obtained best-fit values of β value are tabulated in the Table-6.6. **ANMeNO$_2$** shows absorption saturation along with nonlinear absorption.

Table 6.6: Nonlinear absorption coefficient values of anthracenyl chalcone derivatives.

Compound	β (cm/GW)	Compound	β (cm/GW)	Compound	β (cm/GW)
ANCl	0.49	ANBr	0.76	ANNO$_2$	3.10
ANOMe	2.65	ANH	0.99	ANMeCl	2.57
ANMeBr	4.0	ANMeNO$_2$	5.39	ANMeOMe	0.48
ANMeH	0.31	ANOMeCl	0.60	ANOMeBr	0.89
ANOMeNO$_2$	1.76	ANOMeOMe	1.17	ANOMeH	0.19

To know how the push-pull motifed chalcone affects the nonlinear absorption coefficient (β), and which molecular arrangement can enhance or decrease it, the nonlinear absorption coefficient (β) is plotted as a function of substitution (Scheme 6.2, R = a (–Cl), b (–Br), c (–NO$_2$), d (–OMe), e (–H)) in the chalcone derivatives in the three sub-series with increasing electron donor strength in the anthracenyl 9-position (–H→ –CH$_3$→ –OCH$_3$). In Fig. 6.26 graphically shows the dependence of β with the present structures (**1-15**).

The red line shows the relation between (β) and compounds **6-10**, similiarly, the black line represents the compounds **1-5** and blue lines tells the dependence of **11-15** with β.
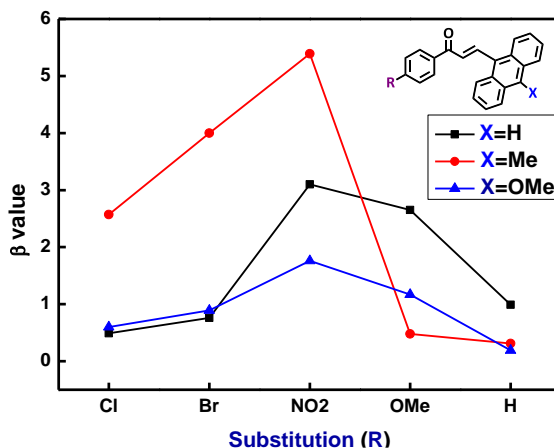
Figure 6.26: β is plotted as a function of substitution in the anthracenyl chalcone derivatives.
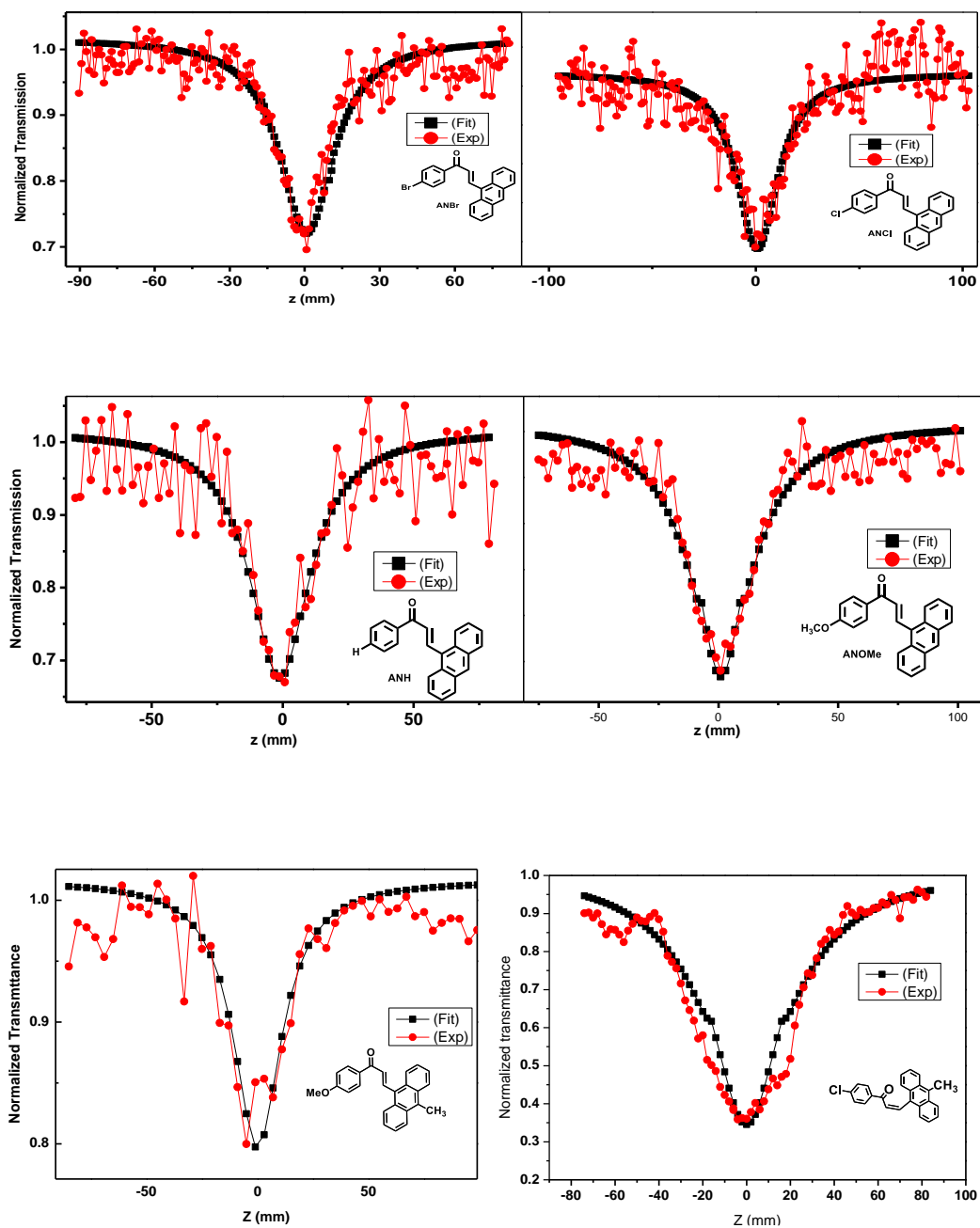
Figure 6.27: Open aperture z scan data of anthracenyl chalcone derivative. Black lines are the best fit to the experimental data using **Eqn.4.3.**
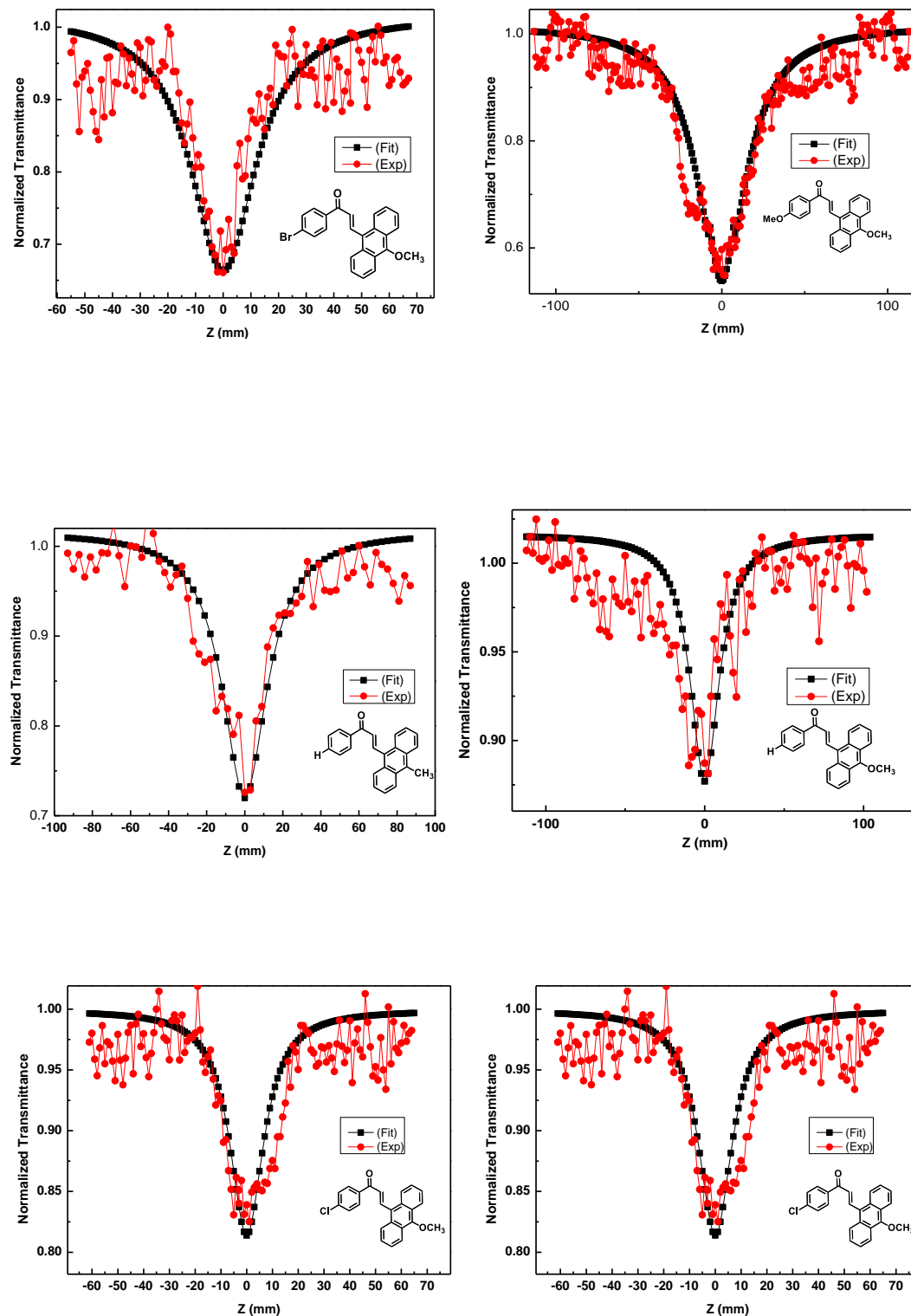
Figure 6.27: Open aperture z scan data of anthracenyl chalcone derivative. Black lines are the best fit to the experimental data using **Eqn.4.3.**

A very regular pattern in the three sub-series was observed. The substituents were changed with usual, but effectual, functional groups like –Cl, –Br, –NO$_2$. The β value increased with –Cl→ –Br→ –NO$_2$ groups, it reached a maximum to -NO$_2$ and decreased to –OMe→–H substitution.

The detailed study to establish the relation between structure and nonlinear absorption coefficient discloses that the +R inductive effect of –CH$_3$ group is much more effective than the electron donating –OCH$_3$ group present in the 9 position of the anthracene moiety. Compound **ANMeCl** & **ANMeBr** have better nonlinear absorption than their other congeners (**ANCl, ANBr, ANOMeCl** and **ANOMeBr**). This observation could be explained by their structural features, presented in Fig. 6.28 a and Fig. 6.28 b.
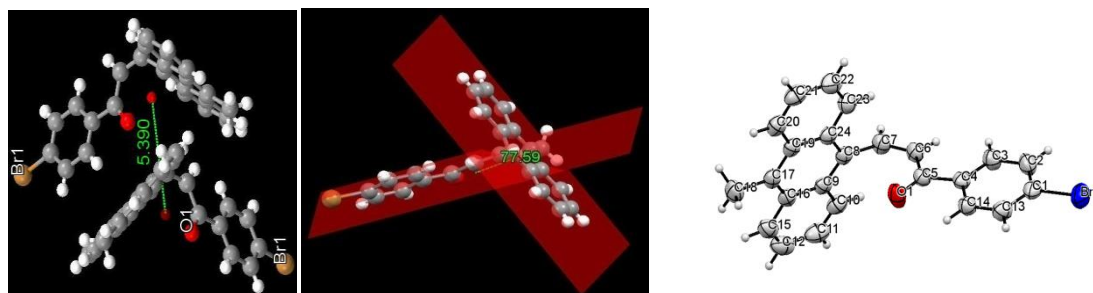
Figure 6.28a: Centroid to Centroid distance; Dihedral angle between the anthracene ring and ethylenic double bond; Numbering system for *(Z)-1-(4-chlorophenyl)-3-(9-methylanthracen-10-yl)prop-2-en-1-one*[ANMeCl].
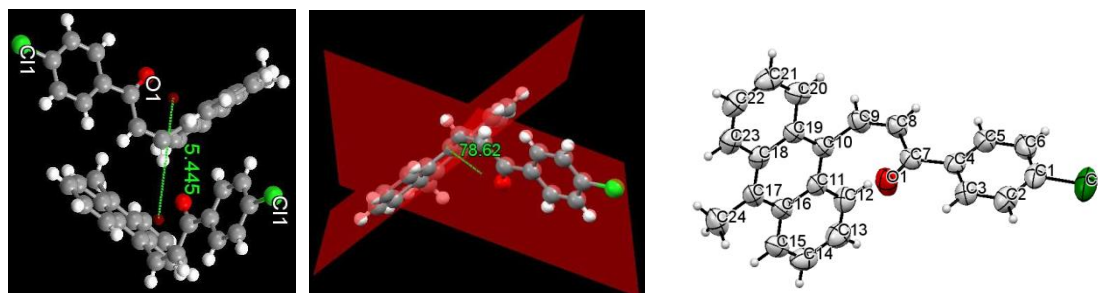
Figure 6.28b: Centroid to Centroid distance; Dihedral angle between the anthracene ring and ethylenic double bond; Numbering system for *(Z)-1-(4-bromoophenyl)-3-(9-methylanthracen-10-yl)prop-2-en-1-one*[ANMeBr].

as (i) both **ANMeCl** and **ANMeBr** have Z configuration as revealed in their single crystal data. The dihedral angle between the anthracene ring and ethylenic double bond for **ANMeCl** and **ANMeBr** is 78.62° and 77.85° respectively (ii) Measured centroid to centroid distance from crystal packing of **ANMeCl** and **ANMeBr** is

5.44 Å and 5.39 Å respectively. Recent study showed that, if the distance is ≈ 6.0 Å, $\pi - \pi$ interaction can be bonding in character [23]. The lower dihedral angle in the *(Z)* conformation compared to the *(E)* conformation of its congener is responsible for the increase in the nonlinear absorption response [24, 25]. The detailed crystal data is given in Table 16.7 and CIF file is provided in the Section 6.12.

Table 16.7: Single crystal XRD data of ANMeCl and ANMeBr.

Data	Compound code		Data	Compound code	
	ANMeCl	**ANMeBr**		**ANMeCl**	**ANMeBr**
Formula	C24H17ClO	C24H17BrO	Z	4	4
Formula weight	356.83	401.28	Density (calculated)	1.336	1.499 g/cm^3
Temperature	296(2)	296(2)	Independent Reflections	3156	5345
Wavelength	0.71073 Å	0.71073 Å	Absorption correction	multi-scan	multi-scan
Crystal Dimensions	a =14.3598(7) Å; b =11.9618(6) Å; c =10.8085(5) Å α = 90.00; β = 107.163(3); γ = 90.00	a =14.4897(17) Å; b =11.9044(14) Å; c =10.7801(13) Å α =90.00; β = 107.021(6); γ = 90.00	Refinement method	full-matrix least-squares refinement on F^2	full-matrix least-squares refinement on F^2
Space group	P 21/c	P 1 21/c 1	Goodness of fit on F2	1.051	1.014
Index ranges	$-17 \leq h \leq 17$ $-13 \leq k \leq 13$ $-12 \leq l \leq 12$	$-20 \leq h \leq 15$ $-16 \leq k \leq 15$ $-15 \leq l \leq 15$	Largest diff. peak and hole	0.311 and -0.488 e$^-$/Å^3	0.931 and -0.825 e$^-$/Å^3
Crystal System	monoclinic	monoclinic	F000	744	816
Volume	1773.89(15) A^{03}	1778.0(4) A^{03}	Theta range for data Collection	1.48- 25.25°	1.47 - 30.34°
Absorption coefficient	0.225 mm^{-1}	2.322 mm^{-1}			

Decrease in β value with electron-donor substituent (-OMe) tells that $A - \pi - A - \pi - D$ is more effective in increasing the nonlinear absorption coefficient than the corresponding $D - \pi - A - \pi - D$ motif in this present study. However, there is a tradeoff between the electron donor moiety and the terminal acceptor group in the motif $A - \pi - A - \pi - D$. The anthracene derivatives having un-substituted 9-position, were much more proficient absorber compared to the methoxy substituted derivatives. Probably the extensive conjugation of the methoxy group with the

anthracene π-system exceeds the "conjugation signature" and in turn decreases the β value [26].

6.10 Conclusion:

A series of eleven chalcones with naphthalene core have been synthesized and characterized. Except, the *(E)-1-(4-substitutedphenyl)-3-(naphthalen-1-yl)prop-2-en-1-one* derivatives, all the compounds had up-conversion photoluminescence properties at 845 nm wavelength. The mechanism behind this is believed to proceed through three photon and two photon absorption. If one keeps in mind the advantages of IR lasers with respect to UV lasers (e.g. reduced cost, wider availability, and more flexible morphology), the potential of such up-converter organic systems in the laser and photonics market becomes clear.

A series *E/Z-3-(9-substituted anthracen-10-yl)-1-(4-substitutedphenyl) prop-2-en-1-one derivatives* (**1-15**) was synthesized using green chemistry and their NLA coefficient was measured by z-scan method using a nanosecond laser. The nonlinearity arises due to fast free-carrier absorption, excited state absorption, and two-photon absorption. The present analysis and interpretation suggest that the +R inductive effect of $-CH_3$ as a donor in the anthracene moiety with terminal electron acceptor $-NO_2$, brings about attractive nonlinear absorption. Most of the synthesized chalcone have extremely large Stokes shift (5215-6743) cm^{-1} and twisted intramolecular charge transfer. Due to the aggregation formation the β value of **ANMeNO₂** must have decreased. Observed results portrayed that *cis* isomer was more effective than the *trans* isomer as the NL absorption coefficient depends on the dihedral angle. A qualitative relationship between the structure and coefficient is unambiguous from this study. As molecules with large Stokes shift eliminates quenching of the fluorescence and gives a stronger signal, the reported compounds have potential use in biological imaging also, most of them could be successfully used as optical sensor due to their NLO properties. Most of the compounds in both the series exhibited NLO property.

6.11 References:

1. Karakurt, A.; Ozalp, M.; Isık, S.; Stables, J.P.; Dalkara, S. *Bioorg. Med. Chem.* **2010**. *18*. 2902.

2. Goksu, S.; Uguz, M.T.; Ozdemir, H.; Secen, H. *Turk J Chem*. **2005**. *29*. 199.

3. Arora, V.; Arora, P.; Lamba, H.S. *Der Pharmacia Lettre*. **2012**. *4(2)*. 554.

4. Batt, D.G.; Maynard, G.D.; Petraitis, J.J.; Shaw, J.E.; Galbraith, W.; Harris, R.R. *J. Med. Chem.* **1990**. *33(1)*. 361.

5. Shin, E.J.; Lee, S.H. *Bull. Korean Chem. Soc.* **2002**. *23(9)*. 1309.

6. Janovec, L.; Suchar, G.; Imrich, J.; Kristian, P.; Sasinkova, V.; Alfoldi, J.; Sedlak, E. *Collect. Czech. Chem. Commun*. **2002**. *67*. 665.

7. Gunnlaugsson, T.; Glynn, M.; Tocci, G.M.; Kruger, P.E.; Pfeffer, F.M. *Coord. Chem. Rev.* **2006**. *250*. 3094.

8. Vogel, A.I.; *Text Book of Practical Organic Chemistry,* ELBS Fourth Edition. **1978**. 762.

9. Minlon, H. *JACS*. **1949**. *71*. 3301.

10. Xue, Y.; Mou, J.; Liu, Y.; Gong, X.; Yang, Y.; Cent, L. *Eur. J. Chem.* **2010** *.8(4)*. 928.

11. Rurack, K.; Bricks, J.L.; Reck, G.; Radeglia, R.; Resch-Genger, U. *J. Phys. Chem. A*. **2000.** *104*. 3087.

12. Shinde, K.N.; Dhoble, S.J.; Swart, H.C.; Park, K. *Phosphate Phosphors for solid-state Lighting*. **2012**. *XIV*. pp. 270; ISBN: 978-3-642-34311-7.

13. Peticolas, W.L.; Goldsborough, J.P. *Phys Rev. Lett.* **1963**. *10*. 43.

14. Abbotto, A.; Beverina, L.; Bozio, R.; Bradamante, S.; Ferrante, C.; Pagani, G. A.; Signorini, R. *Adv. Mater.* **2000**. *12(24)*. 1963.

15. Struve, W.S. *Fundamentals of Molecular Spectroscopy;* John Willey & Sons, Inc.: New York, NY. **1989**.

16. Schutte, C.J.H. *The Theory of Molecular Spectroscopy: The Quantum Mechanics and Group Theory of Vibrating and Rotating Molecules;* North-Holland Publishing Company: Amsterdam, **1976**. *1*.

17. Yariv, A. *Introduction to Optical Electronics;* Holt, Rinehart and Winston: New York, NY. **1976**.

18. Allen, L.; Eberly, J.H. *Optical Resonance and Two-Level Atoms;* John Willey & Sons, Inc.: New York, NY. **1975**.

19. Letokhov, V.S. *Laser Photoionization Spectroscopy;* Academic Press, Inc.: New York, NY. **1978**.

20. Pavia, D.L.; Lampman, M.G.; Kriz, S.G. *Introduction to Spectroscopy*, 3rd Edition, Chapter 7, pp-353-389.

21. Hemmila, I.A. *Applications of Fluorescence in Immunoassays*. Wiley, New York. **1991.**

22. Lavis, L.D.; Raines, R.T. *Curr. Opin. Chem. Biol.* **2008.** *3(3)*. 142.

23. Kruszynski, R.; Sierań ski, T. *Cryst. Growth Des.*

24. Mendis, B.A.S.; De Silva, K.M.N. *Internet Electronic J. Mol. Des.* **2005**. *4 (3)***.** 226.

25. Cheng, L.T.; Tam, W.; Stevenson, S.H.; Meredith, G.R. *J. Phys. Chem.* **1991**. *95.* 10631.

26. Pawlicki, M.; Collins, H.A.; Denning, R.G.; Anderson, H.L. *Angew. Chem. Int. Ed.* **2009**. *48(18)*. 3244.

6.12 Spectral Data of naphthalene and anthracene core chalcones:
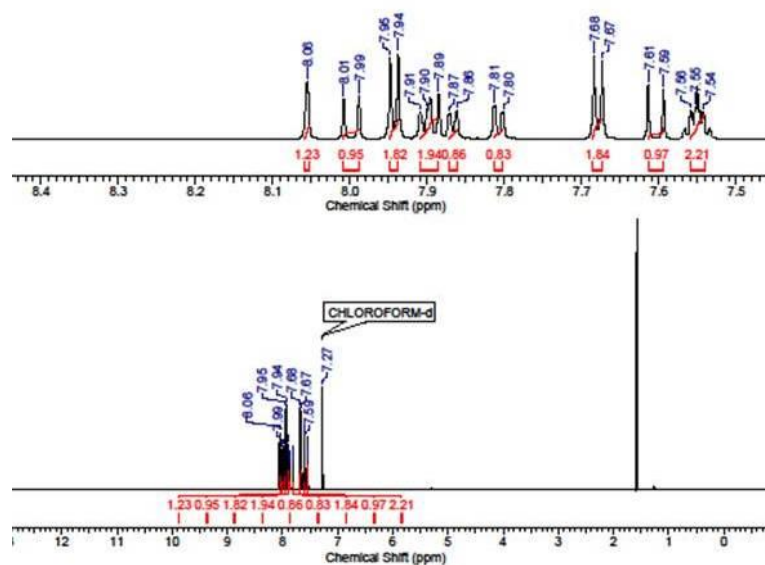
Figure 6.29: ¹H NMR spectrum of *(E)-1-(4-bromophenyl)-3-(naphthalen-1-yl)prop-2-en-1-one* **(F2Br).**
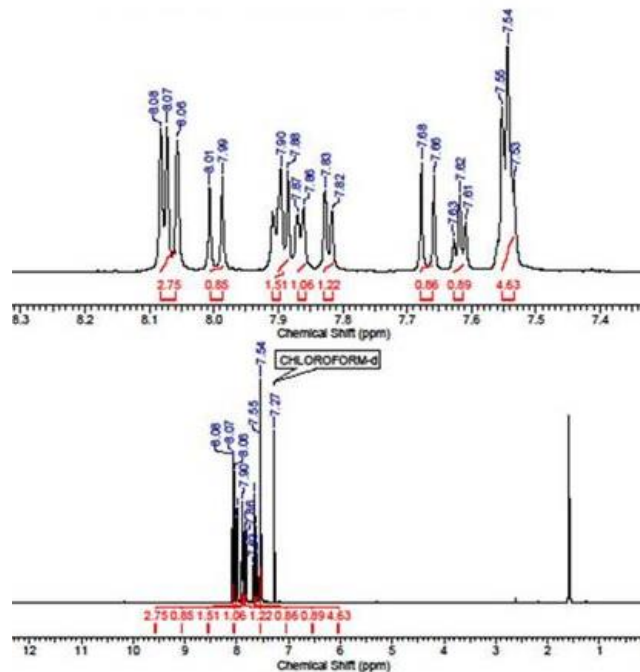
Figure 6.30: ¹H NMR spectrum of *(E)-3-(naphthalen-1-yl)-1-phenylprop-2-en-1-one* **(PS3).**
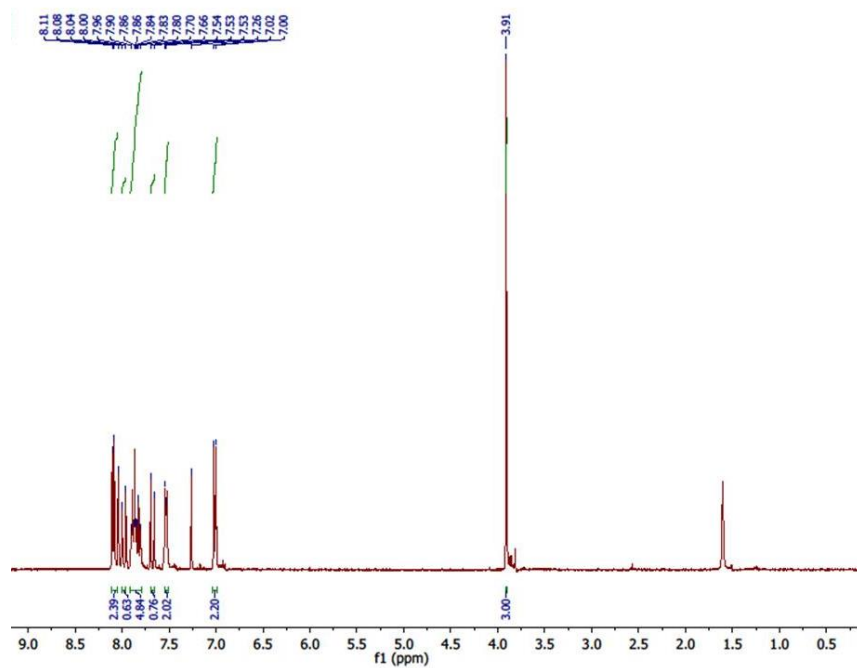
Figure 6.31: ¹H NMR spectrum of *(E)-1-(4-methoxyphenyl)-3-(naphthalen-1-yl)prop-2-en-1-one* **(F2OMe).**
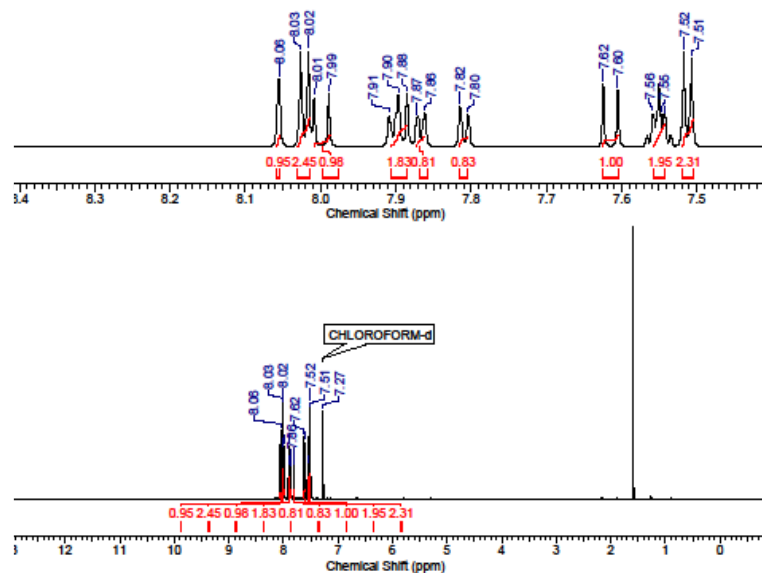
Figure 6.32: ¹H NMR spectrum of *(E)-1-(4-chlorophenyl)-3-(naphthalen-1-yl)prop-2-en-1-one* **(F2Cl).**
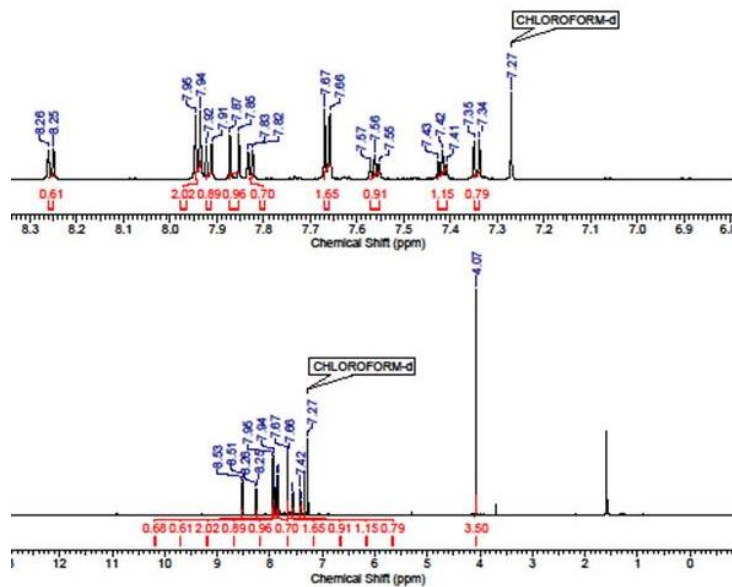
Figure 6.33: ¹H NMR spectrum of *(E)-1-(4-bromophenyl)-3-(4-methoxynaphthalen-1-yl)prop-2-en-1-one* **(NM1Br).**
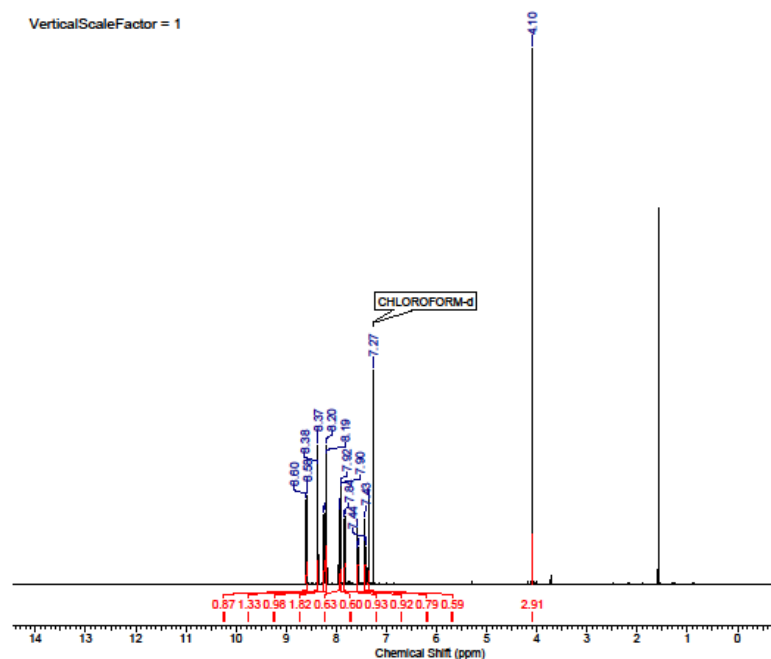
Figure 6.34: ¹H NMR spectrum of *(E)-3-(4-methoxynaphthalen-1-yl)-1-(4-nitrophenyl)prop-2-en-1-one* (NM1NO₂)
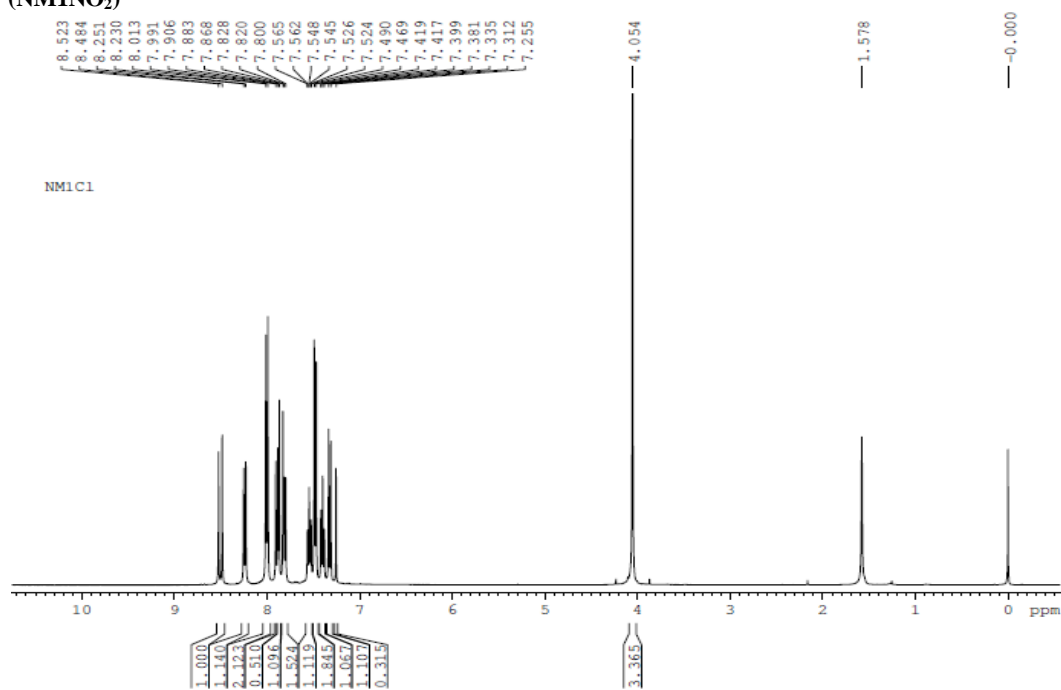
Figure 6.35: ¹H NMR spectrum of *(E)-1-(4-chlorophenyl)-3-(4-methoxynaphthalen-1-yl)prop-2-en-1-one* (NM1Cl).
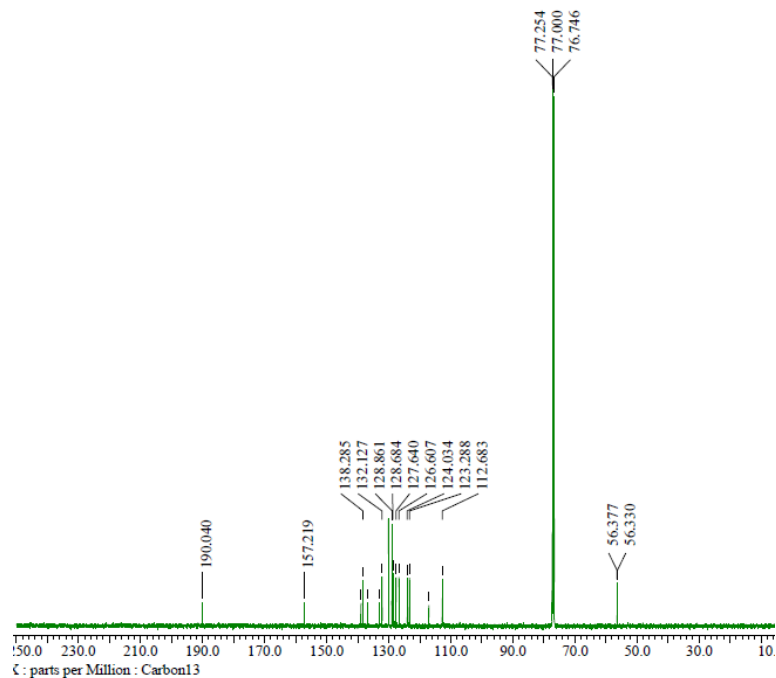
Figure 6.36: ¹³C NMR spectrum of *(E)-1-(4-chlorophenyl)-3-(4-methoxynaphthalen-1-yl)prop-2-en-1-one* (NM1Cl).
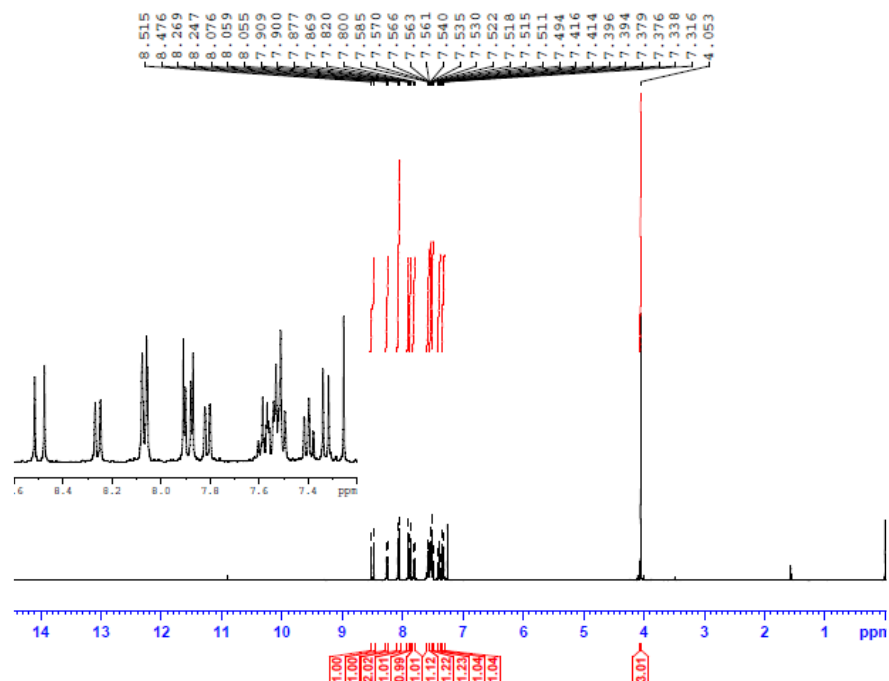
Figure 6.37: ¹H NMR spectrum of *(E)-3-(2-methoxynaphthalen-1-yl)-1-phenylprop-2-en-1-one* (NMH).
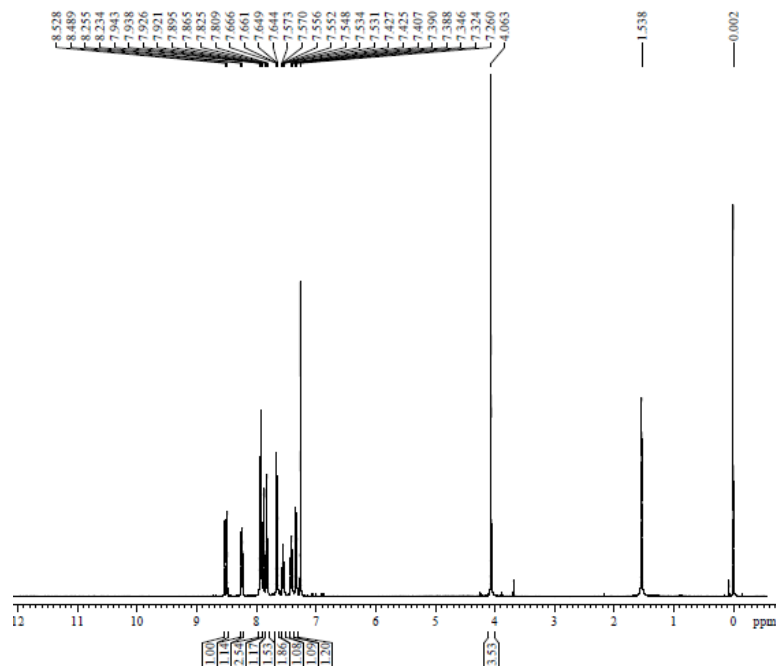
Figure 6.38: ¹H NMR spectrum of *(E)-1-(4-chlorophenyl)-3-(2-methoxynaphthalen-1-yl)prop-2-en-1-one* **(NMCl).**
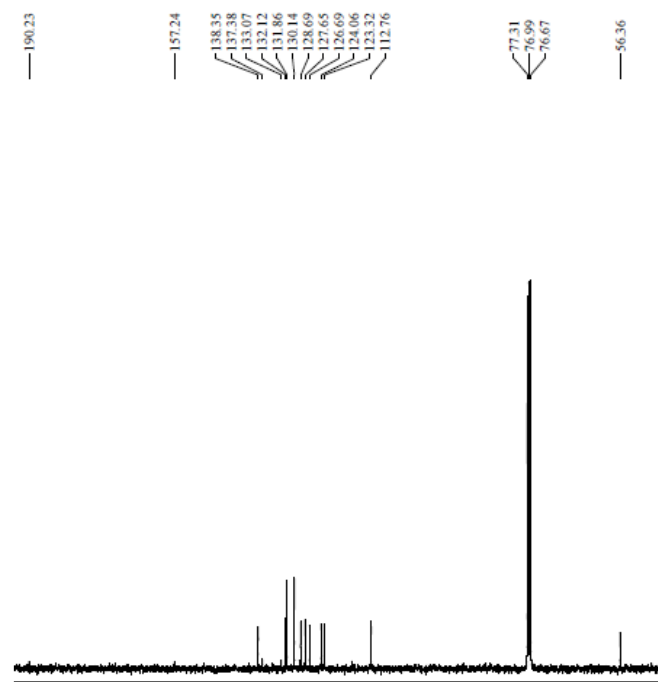
Figure 6.39: ¹³C NMR spectrum of *(E)-1-(4-chlorophenyl)-3-(2-methoxynaphthalen-1-yl)prop-2-en-1-one* **(NMCl).**
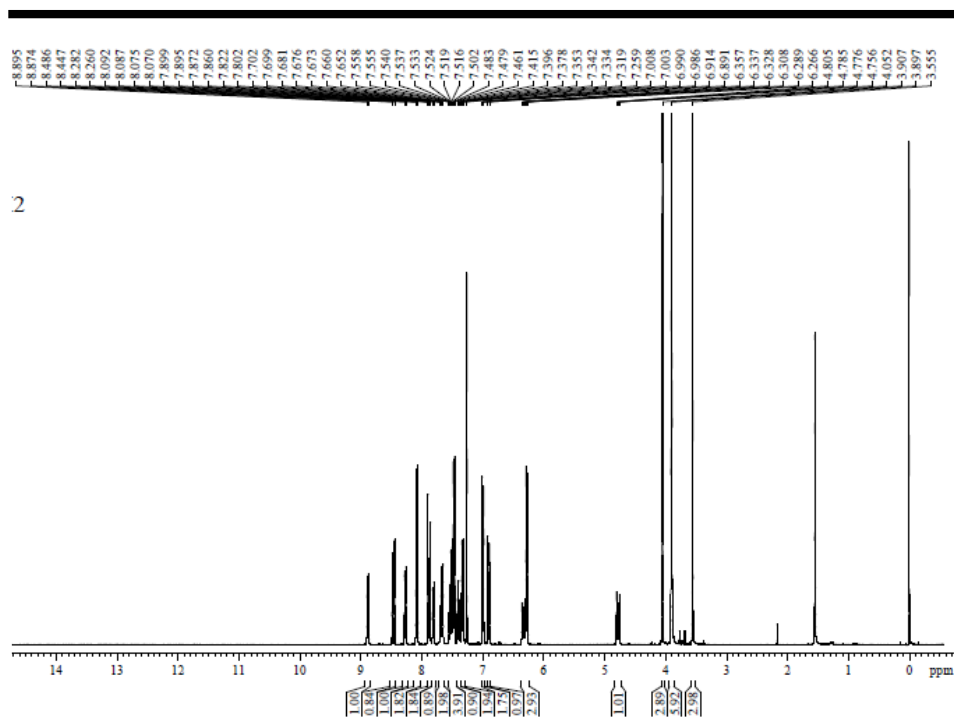
Figure 6.40: ^{1}H NMR spectrum of *(E)-3-(2-methoxynaphthalen-1-yl)-1-(4-methoxyphenyl)prop-2-en-1-one (NM2).*
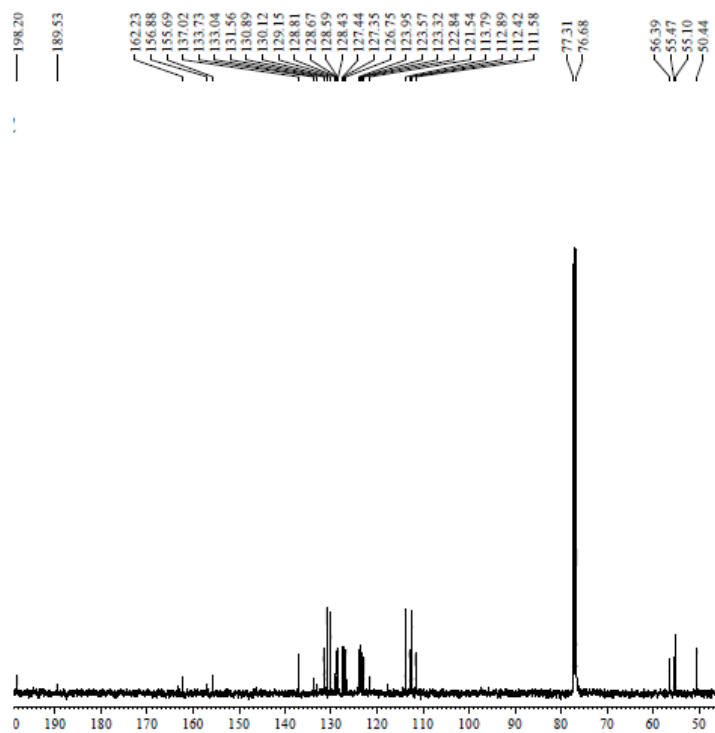
Figure 6.41: ^{13}C NMR spectrum of *(E)-3-(2-methoxynaphthalen-1-yl)-1-(4-methoxyphenyl)prop-2-en-1-one (NM2).*
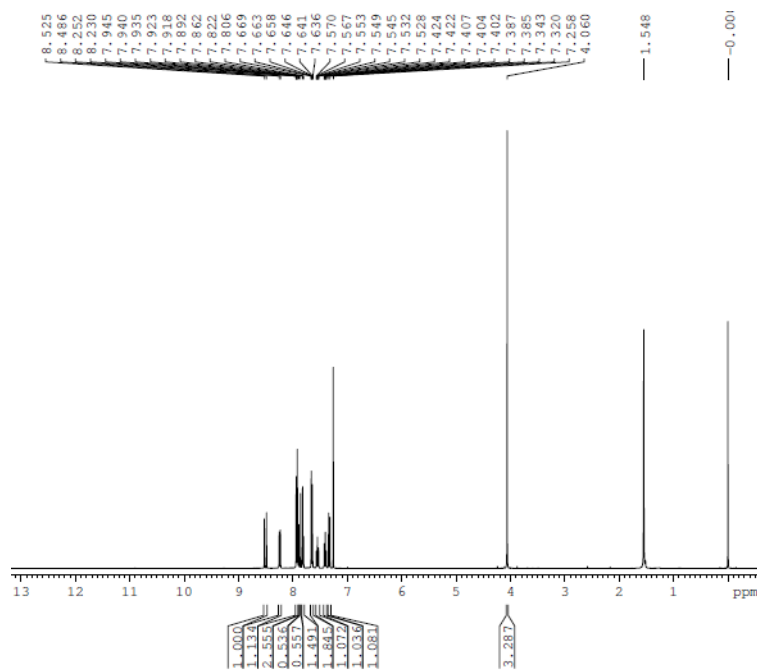
Figure 6.42: ¹H NMR spectrum of *(E)-1-(4-bromophenyl)-3-(2-methoxynaphthalen-1-yl)prop-2-en-1-one* **(NMBr).**
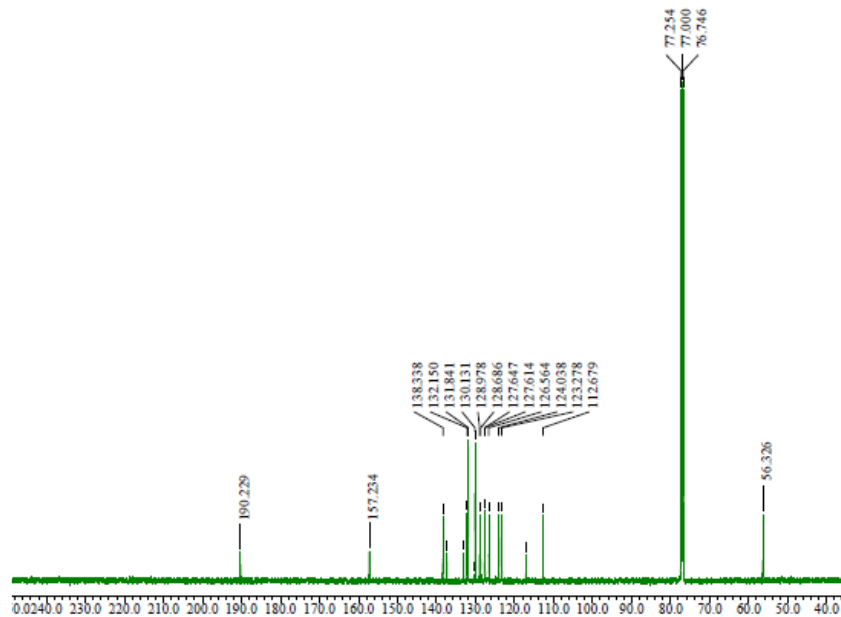
Figure 6.43: ¹³C NMR spectrum of *(E)-1-(4-bromophenyl)-3-(2-methoxynaphthalen-1-yl)prop-2-en-1-one* **(NMBr).**

142
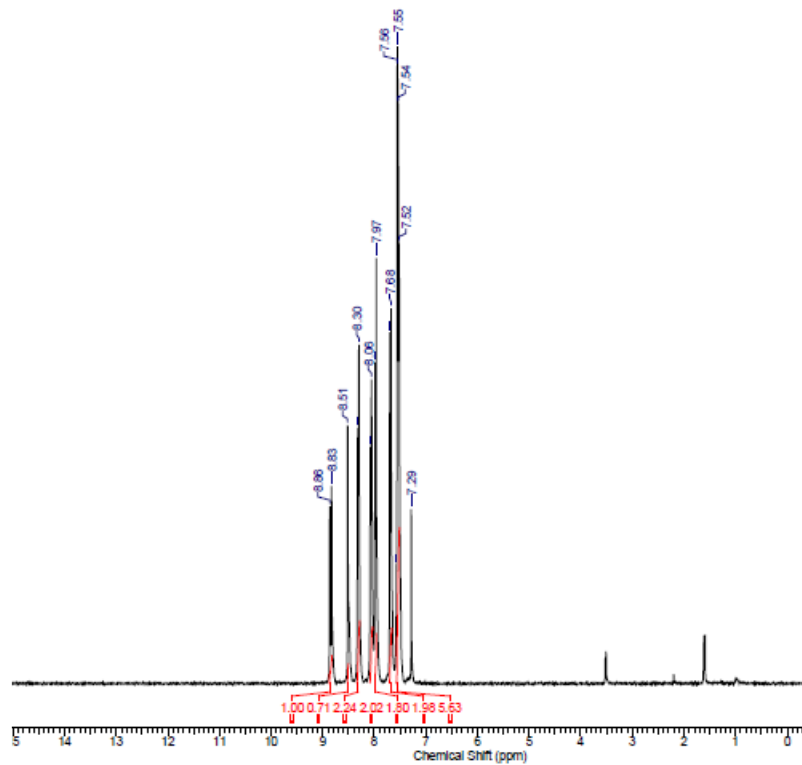
Figure 6.44: ¹H NMR spectrum of *(E)-3-(anthracen-10-yl)-1-(4-bromophenyl)prop-2-en-1-one* **(ANBr).**
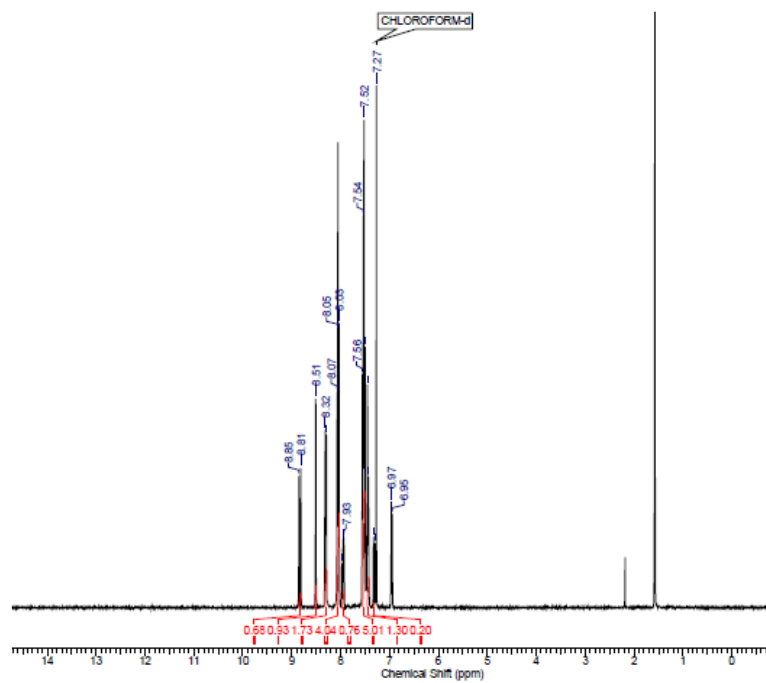
Figure 6.45: ¹H NMR spectrum of *(E)-3-(anthracen-10-yl)-1-(4-chlorophenyl)prop-2-en-1-one* **(ANCl).**
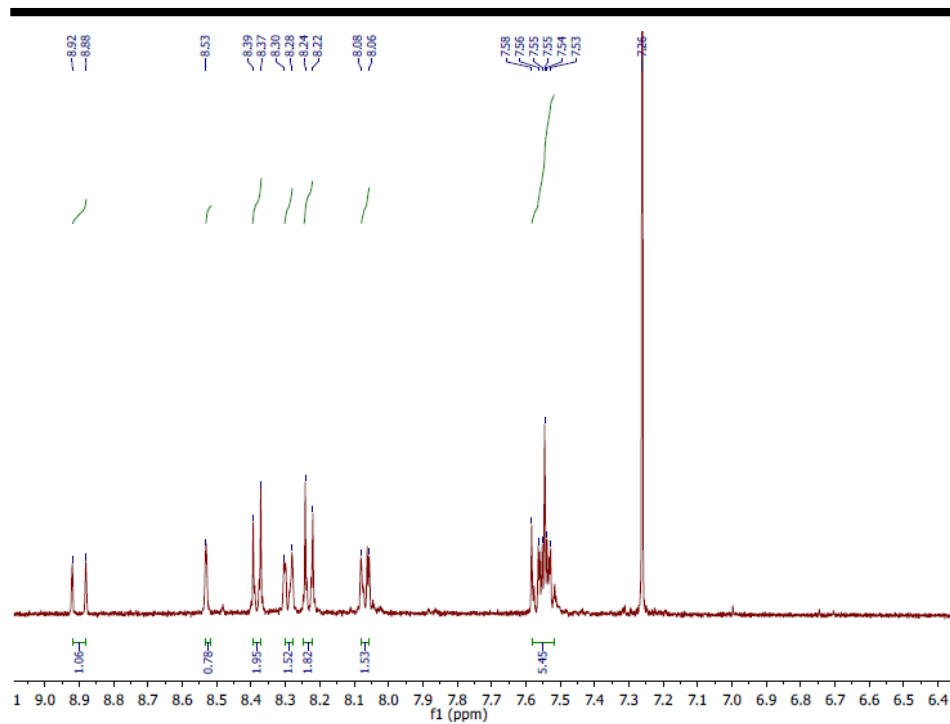
Figure 6.46: **¹H NMR spectrum of** *(E)-3-(anthracen-10-yl)-1-(4-nitrophenyl)prop-2-en-1-one* **(ANNO₂).**
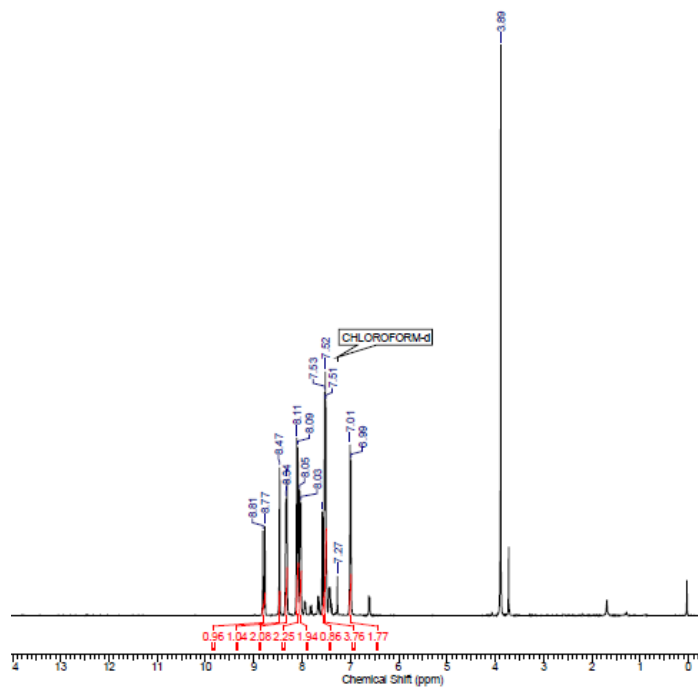
Figure 6.47: **¹H NMR spectrum of** *(E)-3-(anthracen-10-yl)-1-(4-methoxyphenyl)prop-2-en-1-one* **(ANOMe).**
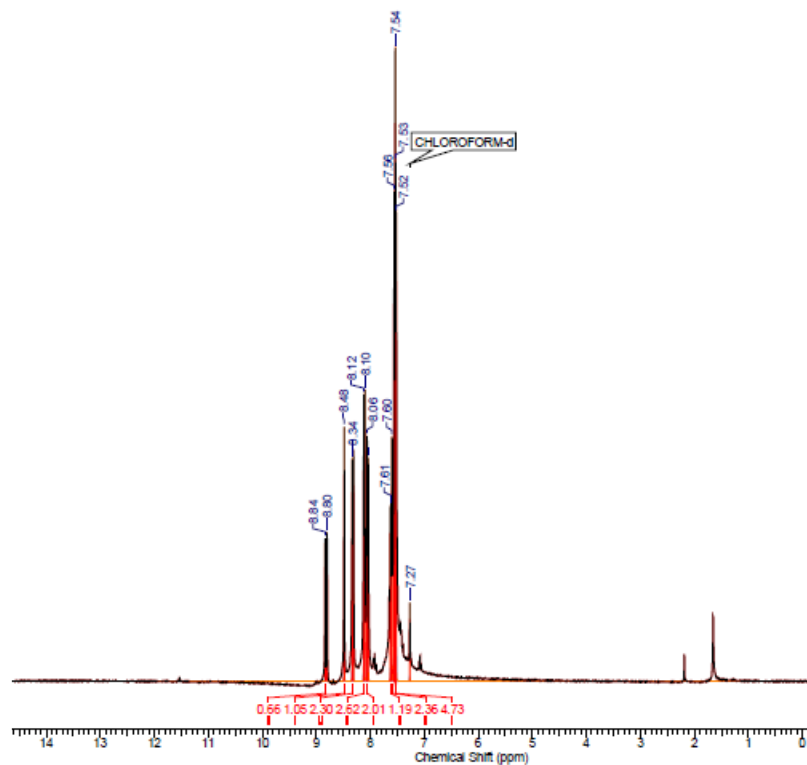
Figure 6.48: ¹H NMR spectrum of *(E)-3-(anthracen-10-yl)-1-phenylprop-2-en-1-one* (ANH).
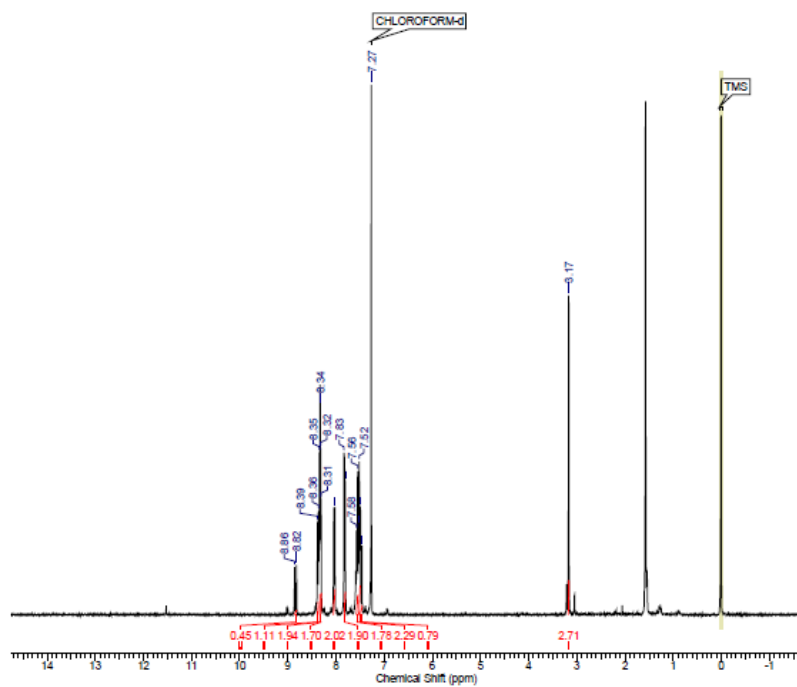
Figure 6.49: ¹H NMR spectrum of *(E)-1-(4-chlorophenyl)-3-(9-methylanthracen-10-yl)prop-2-en-1-one* (ANMeCl).
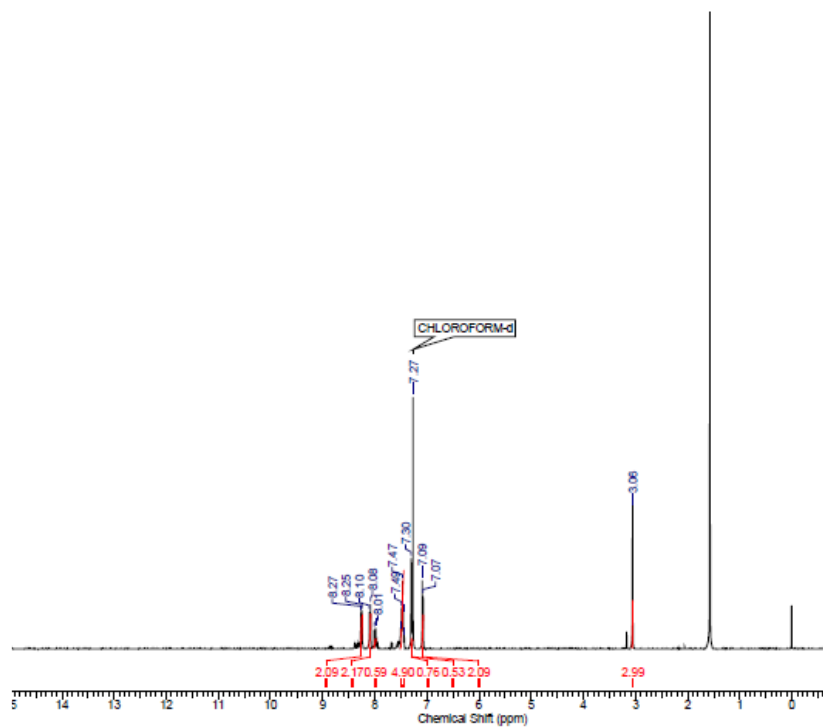
Figure 6.50: ¹H NMR spectrum of *(Z)-1-(4-bromophenyl)-3-(9-methylanthracen-10-yl)prop-2-en-1-one* **(ANMeBr).**
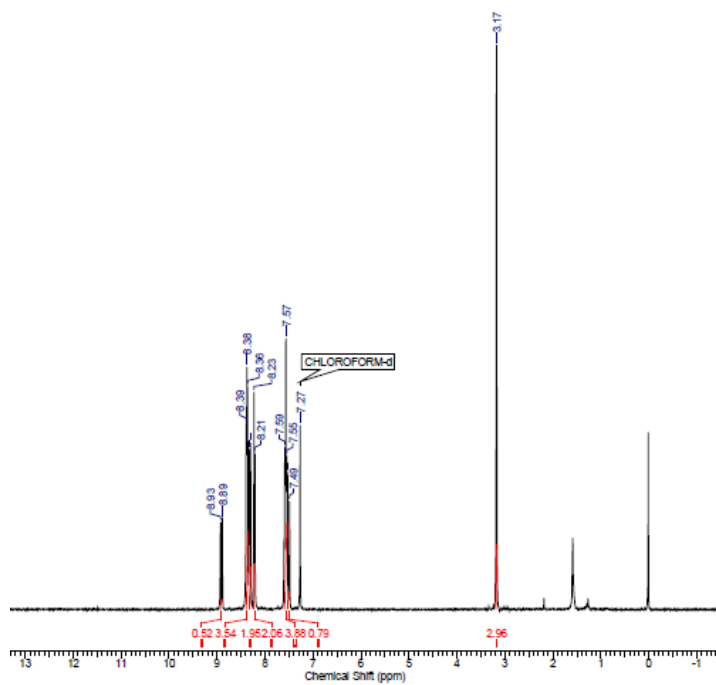
Figure 6.51: ¹H NMR spectrum of *(E)-3-(9-methylanthracen-10-yl)-1-(4-nitrophenyl)prop-2-en-1-one* **(ANMeNO₂).**
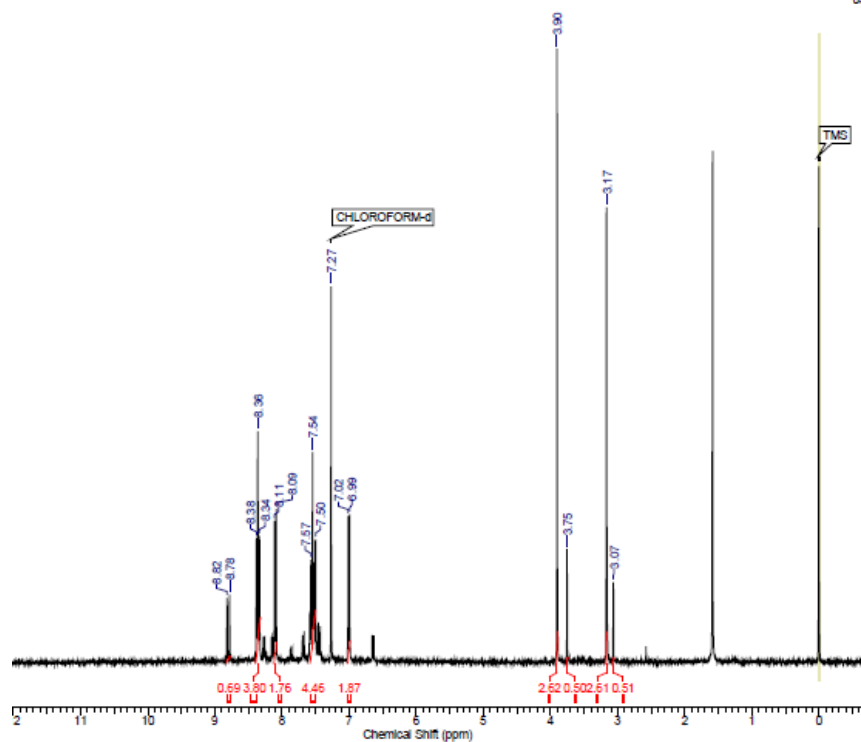
Figure 6.52: ¹H NMR spectrum of *(E)-3-(9-methylanthracen-10-yl)-1-(4-methoxyphenyl)prop-2-en-1-one* (**ANMeOMe**).
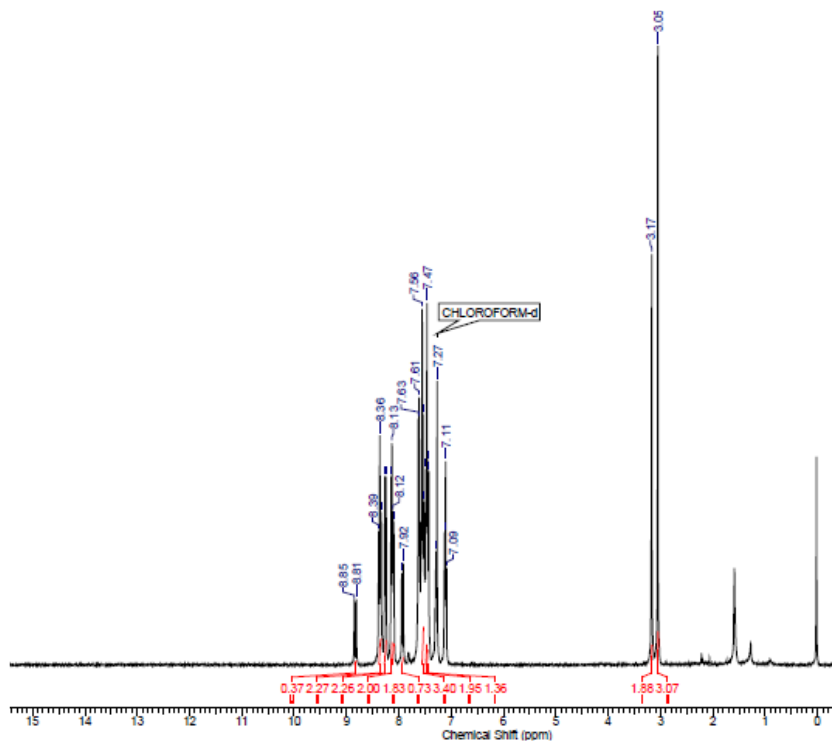
Figure 6.53: ¹H NMR spectrum of *(Z)-3-(9-methylanthracen-10-yl)-1-phenylprop-2-en-1-one* (**ANMeH**).
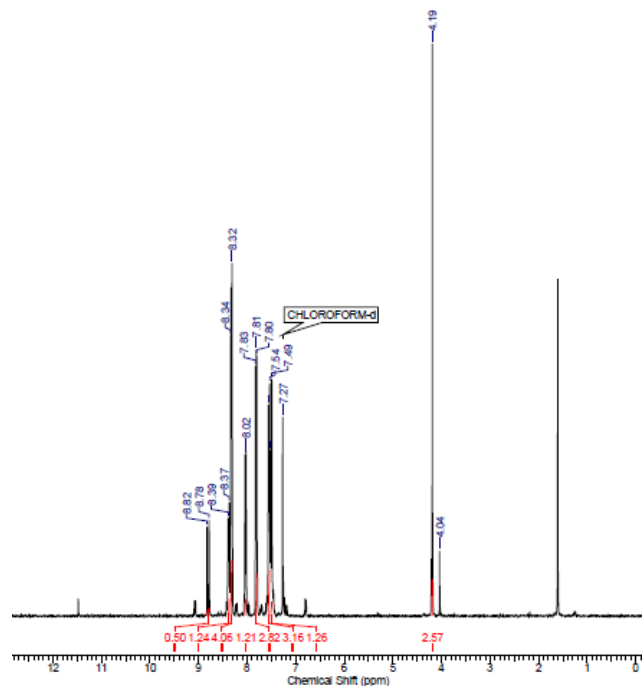
Figure 6.54: ^{1}H NMR spectrum of *(E)-1-(4-chlorophenyl)-3-(9-methoxyanthracen-10-yl)prop-2-en-1-one* (**ANOMeCl**).
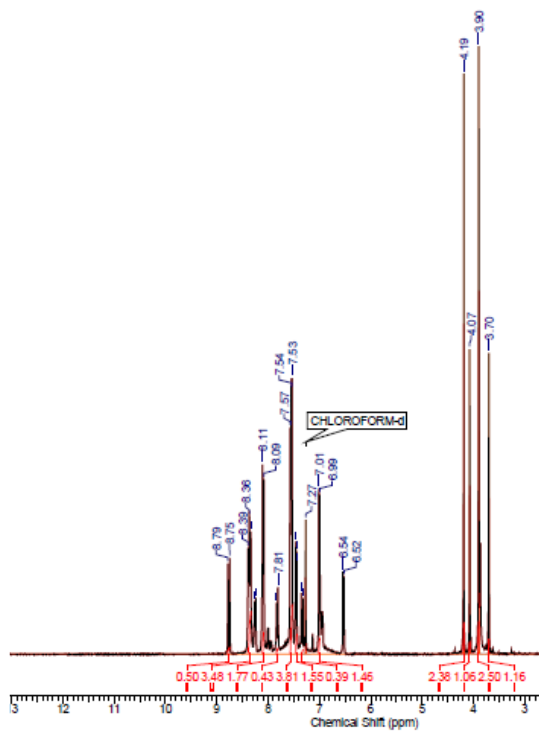

Figure 6.55: ^{1}H NMR spectrum of *(E)-3-(9-methoxyanthracen-10-yl)-1-(4-methoxyphenyl)prop-2-en-1-one* (**ANOMeOMe**).
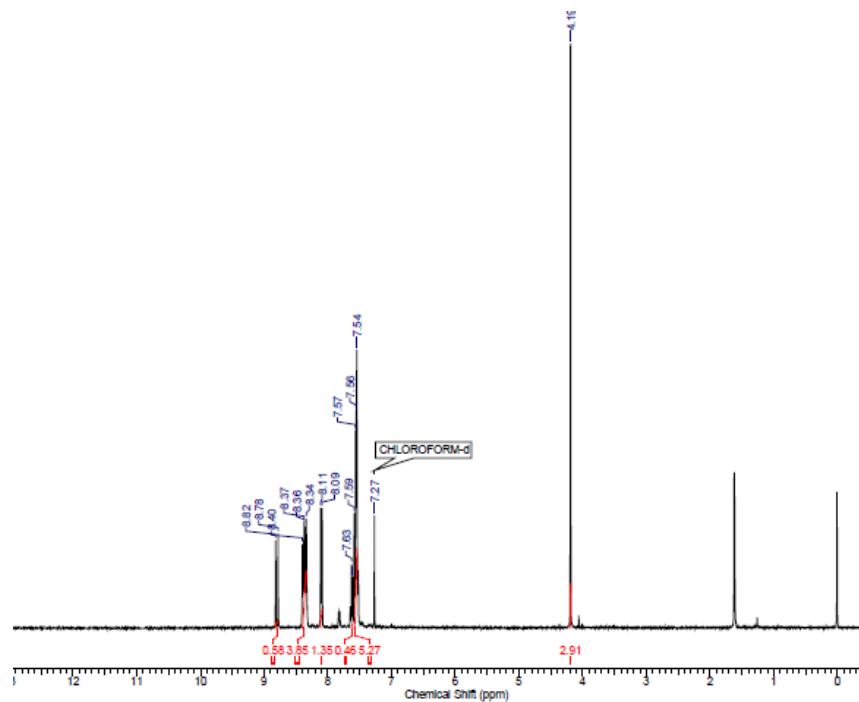
Figure 6.56: ^{1}H NMR spectrum of *(E)-3-(9-methoxyanthracen-10-yl)-1-phenylprop-2-en-1-one* (ANOMeH).
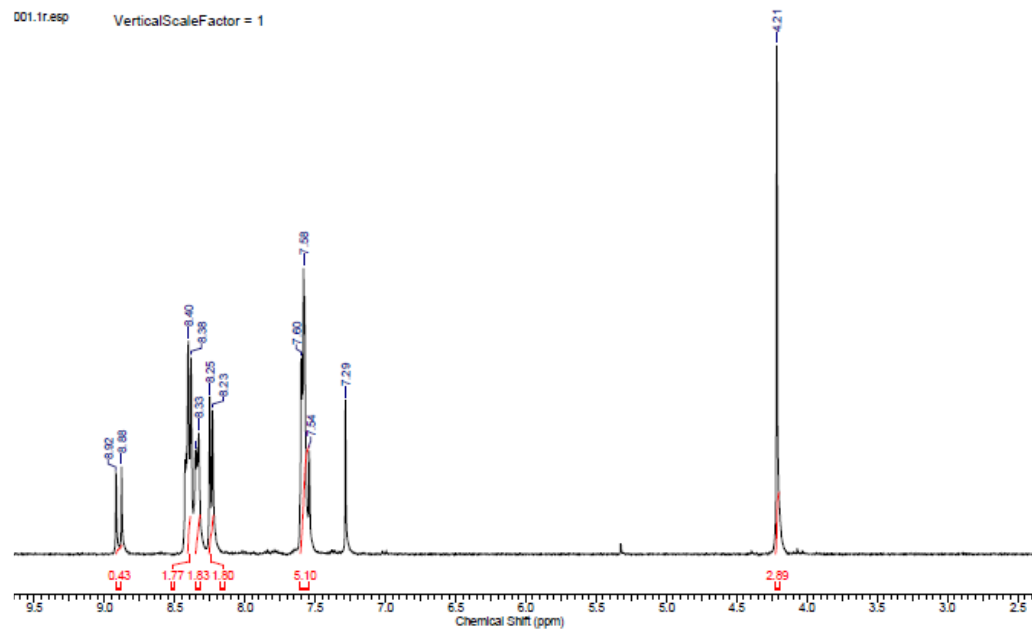
Figure 6.57: ^{1}H NMR spectrum of *(E)-3-(9-methoxyanthracen-10-yl)-1-(4-nitrophenyl)prop-2-en-1-one* (ANOMeNO$_2$).

data_11

_audit_creation_method   SHELXL-97
_chemical_name_systematic
;
 ?
;
_chemical_name_common   ?
_chemical_melting_point   ?
_chemical_formula_moiety   'C24 H17 Cl O'
_chemical_formula_sum   'C24 H17 Cl O'
_chemical_formula_weight   356.83

loop_
 _atom_type_symbol
 _atom_type_description
 _atom_type_scat_dispersion_real
 _atom_type_scat_dispersion_imag
 _atom_type_scat_source
 'C' 'C'   0.0033   0.0016
 'International Tables Vol C Tables 4.2.6.8 and 6.1.1.4'
 'H' 'H'   0.0000   0.0000
 'International Tables Vol C Tables 4.2.6.8 and 6.1.1.4'
 'O' 'O'   0.0106   0.0060
 'International Tables Vol C Tables 4.2.6.8 and 6.1.1.4'
 'Cl' 'Cl'   0.1484   0.1585
 'International Tables Vol C Tables 4.2.6.8 and 6.1.1.4'

_symmetry_cell_setting   monoclinic
_symmetry_space_group_name_H-M   'P 21/c'

loop_
 _symmetry_equiv_pos_as_xyz
 'x, y, z'
 '-x, y+1/2, -z+1/2'
 '-x, -y, -z'
 'x, -y-1/2, z-1/2'

_cell_length_a   14.3598(7)
_cell_length_b   11.9618(6)
_cell_length_c   10.8085(5)
_cell_angle_alpha   90.00
_cell_angle_beta   107.163(3)
_cell_angle_gamma   90.00

```
_cell_volume                    1773.89(15)
_cell_formula_units_Z           4
_cell_measurement_temperature   296(2)
_cell_measurement_reflns_used   2000
_cell_measurement_theta_min     2.36
_cell_measurement_theta_max     25

_exptl_crystal_description      needle
_exptl_crystal_colour           orange
_exptl_crystal_size_max         ?
_exptl_crystal_size_mid         ?
_exptl_crystal_size_min         ?
_exptl_crystal_density_meas     ?
_exptl_crystal_density_diffrn   1.336
_exptl_crystal_density_method   'not measured'
_exptl_crystal_F_000            744
_exptl_absorpt_coefficient_mu   0.225
_exptl_absorpt_correction_type  multi-scan
_exptl_absorpt_correction_T_min 0.937
_exptl_absorpt_correction_T_max 0.957
_exptl_absorpt_process_details  SADABS

_exptl_special_details
;
 ?
;

_diffrn_ambient_temperature     296(2)
_diffrn_radiation_wavelength    0.71073
_diffrn_radiation_type          MoK\a
_diffrn_radiation_source        'fine-focus sealed tube'
_diffrn_radiation_monochromator graphite
_diffrn_measurement_device_type 'CCD area detector'
_diffrn_measurement_method      'phi and omega scans'
_diffrn_detector_area_resol_mean  ?
_diffrn_standards_number        ?
_diffrn_standards_interval_count  ?
_diffrn_standards_interval_time   ?
_diffrn_standards_decay_%       ?
_diffrn_reflns_number           18616
_diffrn_reflns_av_R_equivalents 0.0275
_diffrn_reflns_av_sigmaI/netI   0.0237
_diffrn_reflns_limit_h_min      -17
_diffrn_reflns_limit_h_max      17
_diffrn_reflns_limit_k_min      -13
_diffrn_reflns_limit_k_max      13
```

_diffrn_reflns_limit_l_min   -12
_diffrn_reflns_limit_l_max   12
_diffrn_reflns_theta_min   1.48
_diffrn_reflns_theta_max   25.25
_reflns_number_total   3156
_reflns_number_gt   2203
_reflns_threshold_expression   >2sigma(I)

_computing_data_collection   'Bruker SMART'
_computing_cell_refinement   'Bruker SMART'
_computing_data_reduction   'Bruker SAINT'
_computing_structure_solution   'SHELXS-97 (Sheldrick, 1990)'
_computing_structure_refinement   'SHELXL-97 (Sheldrick, 1997)'
_computing_molecular_graphics   'Bruker SHELXTL'
_computing_publication_material   'Bruker SHELXTL'

_refine_special_details
;
Refinement of F^2 against ALL reflections. The weighted R-factor wR and
goodness of fit S are based on F^2, conventional R-factors R are based
on F, with F set to zero for negative F^2. The threshold expression of
$F^2 > 2sigma(F^2)$ is used only for calculating R-factors(gt) etc. and is
not relevant to the choice of reflections for refinement. R-factors based
on F^2 are statistically about twice as large as those based on F, and R-
factors based on ALL data will be even larger.
;

_refine_ls_structure_factor_coef Fsqd
_refine_ls_matrix_type   full
_refine_ls_weighting_scheme   calc
_refine_ls_weighting_details
'calc w=1/[\s^2^(Fo^2^)+(0.1100P)^2^+0.0000P] where P=(Fo^2^+2Fc^2^)/3'
_atom_sites_solution_primary   direct
_atom_sites_solution_secondary   difmap
_atom_sites_solution_hydrogens   geom
_refine_ls_hydrogen_treatment   mixed
_refine_ls_extinction_method   none
_refine_ls_extinction_coef   ?
_refine_ls_number_reflns   3156
_refine_ls_number_parameters   236
_refine_ls_number_restraints   1
_refine_ls_R_factor_all   0.0701
_refine_ls_R_factor_gt   0.0481
_refine_ls_wR_factor_ref   0.1704
_refine_ls_wR_factor_gt   0.1539
_refine_ls_goodness_of_fit_ref   1.051

_refine_ls_restrained_S_all   1.051
_refine_ls_shift/su_max   0.001
_refine_ls_shift/su_mean   0.000

loop_
 _atom_site_label
 _atom_site_type_symbol
 _atom_site_fract_x
 _atom_site_fract_y
 _atom_site_fract_z
 _atom_site_U_iso_or_equiv
 _atom_site_adp_type
 _atom_site_occupancy
 _atom_site_symmetry_multiplicity
 _atom_site_calc_flag
 _atom_site_refinement_flags
 _atom_site_disorder_assembly
 _atom_site_disorder_group
Cl1 Cl -0.04396(5) 0.22926(6) 0.43935(8) 0.1001(3) Uani 1 1 d . . .
C17 C 0.45722(16) 0.96454(17) 0.65424(18) 0.0542(5) Uani 1 1 d . . .
C18 C 0.51325(14) 0.88056(17) 0.62027(18) 0.0525(5) Uani 1 1 d . . .
C11 C 0.31314(14) 0.89551(16) 0.48343(18) 0.0507(5) Uani 1 1 d . . .
C16 C 0.35725(15) 0.97394(17) 0.58397(17) 0.0508(5) Uani 1 1 d . . .
C7 C 0.24101(14) 0.60366(17) 0.46418(19) 0.0534(5) Uani 1 1 d . . .
C19 C 0.46974(15) 0.80333(17) 0.51781(18) 0.0496(5) Uani 1 1 d . . .
C10 C 0.36959(15) 0.80951(17) 0.45304(17) 0.0492(5) Uani 1 1 d . . .
C5 C 0.12104(16) 0.45827(19) 0.3356(2) 0.0627(6) Uani 1 1 d . . .
H5 H 0.1322 0.4824 0.2594 0.075 Uiso 1 1 calc R . .
C12 C 0.21210(16) 0.9093(2) 0.4147(2) 0.0640(6) Uani 1 1 d . . .
H12 H 0.1823 0.8585 0.3500 0.077 Uiso 1 1 calc R . .
C4 C 0.16968(13) 0.50970(17) 0.45220(18) 0.0498(5) Uani 1 1 d . . .
C9 C 0.32526(17) 0.72812(18) 0.3478(2) 0.0603(6) Uani 1 1 d . . .
H9 H 0.3389 0.7402 0.2700 0.072 Uiso 1 1 calc R . .
C8 C 0.26917(15) 0.64101(17) 0.35030(19) 0.0569(6) Uani 1 1 d . . .
H8 H 0.2457 0.6001 0.2743 0.068 Uiso 1 1 calc R . .
C23 C 0.61587(17) 0.8685(2) 0.6834(2) 0.0675(6) Uani 1 1 d . . .
H23 H 0.6459 0.9161 0.7515 0.081 Uiso 1 1 calc R . .
C15 C 0.29687(19) 1.06106(18) 0.6083(2) 0.0640(6) Uani 1 1 d . . .
H15 H 0.3238 1.1125 0.6736 0.077 Uiso 1 1 calc R . .
C2 C 0.08562(17) 0.38626(19) 0.5599(2) 0.0683(6) Uani 1 1 d . . .
H2 H 0.0736 0.3625 0.6357 0.082 Uiso 1 1 calc R . .
C1 C 0.03897(16) 0.33607(18) 0.4433(2) 0.0649(6) Uani 1 1 d . . .
C21 C 0.62714(19) 0.7164(2) 0.5449(3) 0.0757(7) Uani 1 1 d . . .
H21 H 0.6655 0.6637 0.5196 0.091 Uiso 1 1 calc R . .
C3 C 0.15020(14) 0.47191(17) 0.5630(2) 0.0599(6) Uani 1 1 d . . .
H3 H 0.1817 0.5054 0.6419 0.072 Uiso 1 1 calc R . .

C20 C 0.52985(18) 0.72158(18) 0.4828(2) 0.0642(6) Uani 1 1 d . . .
H20 H 0.5022 0.6712 0.4167 0.077 Uiso 1 1 calc R . .
C14 C 0.20174(19) 1.0713(2) 0.5395(2) 0.0728(7) Uani 1 1 d . . .
H14 H 0.1648 1.1296 0.5573 0.087 Uiso 1 1 calc R . .
C6 C 0.05614(16) 0.37144(19) 0.3315(2) 0.0732(7) Uani 1 1 d . . .
H6 H 0.0244 0.3373 0.2530 0.088 Uiso 1 1 calc R . .
C24 C 0.50198(19) 1.0457(2) 0.7627(2) 0.0770(7) Uani 1 1 d . . .
H24A H 0.4815 1.0268 0.8371 0.115 Uiso 1 1 calc R . .
H24B H 0.4811 1.1202 0.7352 0.115 Uiso 1 1 calc R . .
H24C H 0.5717 1.0414 0.7849 0.115 Uiso 1 1 calc R . .
C22 C 0.66996(18) 0.7898(2) 0.6466(3) 0.0751(7) Uani 1 1 d . . .
H22 H 0.7363 0.7844 0.6893 0.090 Uiso 1 1 calc R . .
C13 C 0.15880(17) 0.9942(2) 0.4413(2) 0.0729(7) Uani 1 1 d . . .
H13 H 0.0935 1.0015 0.3943 0.087 Uiso 1 1 calc R . .
O1 O 0.27715(13) 0.64557(13) 0.57058(14) 0.0795(5) Uani 1 1 d . . .

loop_
 _atom_site_aniso_label
 _atom_site_aniso_U_11
 _atom_site_aniso_U_22
 _atom_site_aniso_U_33
 _atom_site_aniso_U_23
 _atom_site_aniso_U_13
 _atom_site_aniso_U_12
Cl1 0.0715(5) 0.0767(6) 0.1460(8) 0.0074(4) 0.0225(4) -0.0176(3)
C17 0.0739(14) 0.0517(13) 0.0391(11) 0.0032(9) 0.0199(10) -0.0116(11)
C18 0.0601(12) 0.0552(13) 0.0425(11) 0.0106(9) 0.0154(9) -0.0084(10)
C11 0.0614(12) 0.0474(12) 0.0459(11) 0.0082(9) 0.0199(9) -0.0047(10)
C16 0.0698(13) 0.0433(12) 0.0450(11) 0.0051(9) 0.0256(10) -0.0046(10)
C7 0.0565(12) 0.0530(13) 0.0476(13) -0.0047(10) 0.0108(9) 0.0011(10)
C19 0.0614(12) 0.0479(12) 0.0424(11) 0.0082(9) 0.0196(9) -0.0008(10)
C10 0.0648(13) 0.0443(12) 0.0408(11) 0.0023(8) 0.0191(9) -0.0027(10)
C5 0.0626(13) 0.0657(15) 0.0608(14) -0.0076(11) 0.0197(10) -0.0055(11)
C12 0.0609(13) 0.0596(14) 0.0685(14) 0.0036(11) 0.0146(11) -0.0034(11)
C4 0.0477(11) 0.0499(13) 0.0499(12) -0.0022(9) 0.0112(9) 0.0058(9)
C9 0.0771(15) 0.0582(15) 0.0470(12) -0.0022(10) 0.0207(11) -0.0056(12)
C8 0.0665(13) 0.0564(14) 0.0461(12) -0.0064(9) 0.0143(10) -0.0036(11)
C23 0.0661(14) 0.0783(17) 0.0566(13) 0.0136(11) 0.0155(11) -0.0100(13)
C15 0.0933(17) 0.0473(14) 0.0609(14) 0.0020(10) 0.0375(12) -0.0010(12)
C2 0.0622(13) 0.0690(16) 0.0739(16) 0.0160(13) 0.0204(12) 0.0037(13)
C1 0.0517(12) 0.0520(14) 0.0885(18) 0.0051(12) 0.0169(12) 0.0022(10)
C21 0.0736(16) 0.0820(19) 0.0792(18) 0.0224(14) 0.0346(14) 0.0235(14)
C3 0.0592(13) 0.0584(14) 0.0602(13) 0.0014(10) 0.0145(10) 0.0003(11)
C20 0.0822(16) 0.0573(15) 0.0581(14) 0.0092(10) 0.0284(12) 0.0094(12)
C14 0.0842(17) 0.0623(16) 0.0826(17) 0.0130(13) 0.0410(14) 0.0154(13)
C6 0.0623(14) 0.0695(17) 0.0807(17) -0.0208(13) 0.0102(12) -0.0052(12)

C24 0.0947(18) 0.0670(16) 0.0636(16) -0.0080(12) 0.0146(13) -0.0157(13)
C22 0.0614(14) 0.092(2) 0.0706(17) 0.0258(15) 0.0184(13) 0.0026(14)
C13 0.0627(14) 0.0736(18) 0.0833(17) 0.0112(14) 0.0231(12) 0.0069(13)
O1 0.0985(12) 0.0875(12) 0.0507(10) -0.0105(8) 0.0192(8) -0.0353(10)

_geom_special_details
;
 All esds (except the esd in the dihedral angle between two l.s. planes)
 are estimated using the full covariance matrix. The cell esds are taken
 into account individually in the estimation of esds in distances, angles
 and torsion angles; correlations between esds in cell parameters are only
 used when they are defined by crystal symmetry. An approximate (isotropic)
 treatment of cell esds is used for estimating esds involving l.s. planes.
;

loop_
 _geom_bond_atom_site_label_1
 _geom_bond_atom_site_label_2
 _geom_bond_distance
 _geom_bond_site_symmetry_2
 _geom_bond_publ_flag
Cl1 C1 1.739(2) . ?
C17 C18 1.402(3) . ?
C17 C16 1.417(3) . ?
C17 C24 1.512(3) . ?
C18 C19 1.436(3) . ?
C18 C23 1.437(3) . ?
C11 C10 1.407(3) . ?
C11 C12 1.431(3) . ?
C11 C16 1.434(3) . ?
C16 C15 1.429(3) . ?
C7 O1 1.221(2) . ?
C7 C8 1.474(3) . ?
C7 C4 1.500(3) . ?
C19 C10 1.403(3) . ?
C19 C20 1.427(3) . ?
C10 C9 1.490(3) . ?
C5 C6 1.387(3) . ?
C5 C4 1.391(3) . ?
C12 C13 1.353(3) . ?
C4 C3 1.383(2) . ?
C9 C8 1.322(3) . ?
C23 C22 1.353(3) . ?
C15 C14 1.355(3) . ?
C2 C3 1.376(3) . ?
C2 C1 1.378(3) . ?

C1 C6 1.370(3) . ?
C21 C20 1.361(3) . ?
C21 C22 1.399(4) . ?
C14 C13 1.404(3) . ?

loop_
 _geom_angle_atom_site_label_1
 _geom_angle_atom_site_label_2
 _geom_angle_atom_site_label_3
 _geom_angle
 _geom_angle_site_symmetry_1
 _geom_angle_site_symmetry_3
 _geom_angle_publ_flag
C18 C17 C16 119.05(18) . . ?
C18 C17 C24 121.2(2) . . ?
C16 C17 C24 119.8(2) . . ?
C17 C18 C19 120.68(18) . . ?
C17 C18 C23 122.4(2) . . ?
C19 C18 C23 117.0(2) . . ?
C10 C11 C12 121.90(19) . . ?
C10 C11 C16 119.94(18) . . ?
C12 C11 C16 118.14(19) . . ?
C17 C16 C15 122.22(19) . . ?
C17 C16 C11 120.36(18) . . ?
C15 C16 C11 117.4(2) . . ?
O1 C7 C8 121.14(19) . . ?
O1 C7 C4 118.58(17) . . ?
C8 C7 C4 120.24(17) . . ?
C10 C19 C20 120.98(19) . . ?
C10 C19 C18 119.96(18) . . ?
C20 C19 C18 119.06(19) . . ?
C19 C10 C11 119.88(18) . . ?
C19 C10 C9 119.38(18) . . ?
C11 C10 C9 120.67(18) . . ?
C6 C5 C4 120.8(2) . . ?
C13 C12 C11 121.8(2) . . ?
C3 C4 C5 117.65(19) . . ?
C3 C4 C7 118.51(17) . . ?
C5 C4 C7 123.84(18) . . ?
C8 C9 C10 128.72(19) . . ?
C9 C8 C7 125.07(19) . . ?
C22 C23 C18 121.8(2) . . ?
C14 C15 C16 122.2(2) . . ?
C3 C2 C1 119.3(2) . . ?
C6 C1 C2 120.5(2) . . ?
C6 C1 Cl1 120.38(18) . . ?

C2 C1 Cl1 119.16(19) . . ?
C20 C21 C22 120.6(2) . . ?
C2 C3 C4 122.0(2) . . ?
C21 C20 C19 120.9(2) . . ?
C15 C14 C13 120.2(2) . . ?
C1 C6 C5 119.8(2) . . ?
C23 C22 C21 120.7(2) . . ?
C12 C13 C14 120.3(2) . . ?

_diffrn_measured_fraction_theta_max   0.980
_diffrn_reflns_theta_full   25.25
_diffrn_measured_fraction_theta_full   0.980
_refine_diff_density_max   0.311
_refine_diff_density_min   -0.488
_refine_diff_density_rms   0.074

CIF File data of ANMeBr:

data_qq

_audit_creation_method   SHELXL-97

_chemical_name_systematic

;

 ?

;

_chemical_name_common   ?

_chemical_melting_point   ?

_chemical_formula_moiety   'C24 H17 Br O'

_chemical_formula_sum

'C24 H17 Br O'

_chemical_formula_weight   401.28

loop_

 _atom_type_symbol

 _atom_type_description

 _atom_type_scat_dispersion_real

 _atom_type_scat_dispersion_imag

 _atom_type_scat_source

'C' 'C'   0.0033   0.0016

'International Tables Vol C Tables 4.2.6.8 and 6.1.1.4'

'H' 'H'   0.0000   0.0000

'International Tables Vol C Tables 4.2.6.8 and 6.1.1.4'

'O' 'O'   0.0106   0.0060

'International Tables Vol C Tables 4.2.6.8 and 6.1.1.4'

'Br' 'Br' -0.2901   2.4595

'International Tables Vol C Tables 4.2.6.8 and 6.1.1.4'

_symmetry_cell_setting   monoclinic

_symmetry_space_group_name_H-M   'P 21/c'

loop_

 _symmetry_equiv_pos_as_xyz

 'x, y, z'

 '-x, y+1/2, -z+1/2'

 '-x, -y, -z'

 'x, -y-1/2, z-1/2'

_cell_length_a   14.4897(17)

_cell_length_b   11.9044(14)

_cell_length_c   10.7801(13)

_cell_angle_alpha   90.00

_cell_angle_beta   107.021(6)

_cell_angle_gamma   90.00

_cell_volume   1778.0(4)

_cell_formula_units_Z   4

_cell_measurement_temperature   296(2)

_cell_measurement_reflns_used   2000

_cell_measurement_theta_min   10

_cell_measurement_theta_max   25

_exptl_crystal_description   plate

_exptl_crystal_colour   orange

_exptl_crystal_size_max   0.41

_exptl_crystal_size_mid   0.22

_exptl_crystal_size_min   0.14

_exptl_crystal_density_meas   ?

_exptl_crystal_density_diffrn   1.499

_exptl_crystal_density_method   'not measured'

_exptl_crystal_F_000   816

_exptl_absorpt_coefficient_mu   2.322

_exptl_absorpt_correction_type   multi-scan

_exptl_absorpt_correction_T_min   0.547

_exptl_absorpt_correction_T_max   0.722

_exptl_absorpt_process_details   'SADABS;Sheldrick,1996'

_exptl_special_details

;

 ?

;

_diffrn_ambient_temperature   296(2)

_diffrn_radiation_wavelength   0.71073

_diffrn_radiation_type   MoK\a

_diffrn_radiation_source   'fine-focus sealed tube'

_diffrn_radiation_monochromator   graphite

_diffrn_measurement_device_type 'Bruker Smart Apex II'

_diffrn_measurement_method   '\w and \F'

_diffrn_detector_area_resol_mean ?

_diffrn_reflns_number   19739

_diffrn_reflns_av_R_equivalents   0.0312

_diffrn_reflns_av_sigmaI/netI   0.0388

_diffrn_reflns_limit_h_min   -20

_diffrn_reflns_limit_h_max   15

_diffrn_reflns_limit_k_min   -16

_diffrn_reflns_limit_k_max   15

_diffrn_reflns_limit_l_min   -15

_diffrn_reflns_limit_l_max   15

_diffrn_reflns_theta_min   1.47

_diffrn_reflns_theta_max   30.34

_reflns_number_total   5345

_reflns_number_gt   3185

_reflns_threshold_expression   >2sigma(I)

_computing_data_collection   ?

_computing_cell_refinement   ?

_computing_data_reduction   ?

_computing_structure_solution   'SHELXS-97 (Sheldrick, 2008)'

_computing_structure_refinement   'SHELXL-97 (Sheldrick, 2008)'

_computing_molecular_graphics   ?

_computing_publication_material   ?

_refine_special_details

;

Refinement of F^2 against ALL reflections. The weighted R-factor wR and

goodness of fit S are based on F^2, conventional R-factors R are based

on F, with F set to zero for negative F^2. The threshold expression of

$F^2 > 2sigma(F^2)$ is used only for calculating R-factors(gt) etc. and is

not relevant to the choice of reflections for refinement. R-factors based

on F^2 are statistically about twice as large as those based on F, and R-

factors based on ALL data will be even larger.

;

_refine_ls_structure_factor_coef Fsqd

_refine_ls_matrix_type   full

_refine_ls_weighting_scheme   calc

_refine_ls_weighting_details

'calc w=1/[\s^2^(Fo^2^)+(0.0543P)^2^+1.0465P] where P=(Fo^2^+2Fc^2^)/3'

_atom_sites_solution_primary   direct

_atom_sites_solution_secondary   difmap

_atom_sites_solution_hydrogens   geom

_refine_ls_hydrogen_treatment   riding

_refine_ls_extinction_method   none

_refine_ls_extinction_coef   ?

_refine_ls_number_reflns   5243

_refine_ls_number_parameters   236

_refine_ls_number_restraints   0

_refine_ls_R_factor_all   0.0922

_refine_ls_R_factor_gt   0.0472

_refine_ls_wR_factor_ref   0.1334

_refine_ls_wR_factor_gt   0.1150

_refine_ls_goodness_of_fit_ref   1.014

_refine_ls_restrained_S_all   1.014

_refine_ls_shift/su_max   0.003

_refine_ls_shift/su_mean   0.000

loop_

 _atom_site_label

 _atom_site_type_symbol

 _atom_site_fract_x

 _atom_site_fract_y

 _atom_site_fract_z

 _atom_site_U_iso_or_equiv

 _atom_site_adp_type

 _atom_site_occupancy

 _atom_site_symmetry_multiplicity

 _atom_site_calc_flag

 _atom_site_refinement_flags

 _atom_site_disorder_assembly

 _atom_site_disorder_group

Br1 Br 0.45091(2) 1.27432(3) -0.06059(4) 0.07532(16) Uani 1 1 d . . .

O1 O 0.78308(16) 0.85542(18) 0.07120(16) 0.0633(6) Uani 1 1 d . . .

C1 C 0.54249(18) 1.1599(2) -0.0563(3) 0.0495(6) Uani 1 1 d . . .

C2 C 0.5603(2) 1.1259(2) -0.1685(3) 0.0574(7) Uani 1 1 d . . .

H2 H 0.5284 1.1598 -0.2471 0.069 Uiso 1 1 calc R . .

C3 C 0.6263(2) 1.0407(2) -0.1639(2) 0.0510(6) Uani 1 1 d . . .

H3 H 0.6383 1.0173 -0.2400 0.061 Uiso 1 1 calc R . .

C4 C 0.67444(17) 0.9897(2) -0.0475(2) 0.0398(5) Uani 1 1 d . . .

C5 C 0.74695(18) 0.8971(2) -0.0346(2) 0.0415(5) Uani 1 1 d . . .

C6 C 0.77467(19) 0.8606(2) -0.1494(2) 0.0452(6) Uani 1 1 d . . .

H6 H 0.7516 0.9024 -0.2251 0.054 Uiso 1 1 calc R . .

C7 C 0.8302(2) 0.7726(2) -0.1527(2) 0.0485(6) Uani 1 1 d . . .

H7 H 0.8445 0.7609 -0.2303 0.058 Uiso 1 1 calc R . .

C8 C 0.87209(18) 0.6908(2) -0.0479(2) 0.0400(5) Uani 1 1 d . . .

C9 C 0.97128(18) 0.6962(2) 0.0178(2) 0.0402(5) Uani 1 1 d . . .

C10 C 1.0318(2) 0.7771(2) -0.0156(3) 0.0522(7) Uani 1 1 d . . .

H10 H 1.0054 0.8278 -0.0821 0.063 Uiso 1 1 calc R . .

C11 C 1.1272(2) 0.7820(3) 0.0475(3) 0.0635(8) Uani 1 1 d . . .

H11 H 1.1658 0.8348 0.0227 0.076 Uiso 1 1 calc R . .

C12 C 1.1685(2) 0.7080(3) 0.1500(3) 0.0648(8) Uani 1 1 d . . .

H12 H 1.2340 0.7129 0.1938 0.078 Uiso 1 1 calc R . .

C13 C 0.5891(2) 1.1103(2) 0.0609(3) 0.0533(6) Uani 1 1 d . . .

H13 H 0.5764 1.1335 0.1367 0.064 Uiso 1 1 calc R . .

C14 C 0.65450(18) 1.0260(2) 0.0640(2) 0.0463(6) Uani 1 1 d . . .

H14 H 0.6862 0.9925 0.1430 0.056 Uiso 1 1 calc R . .

C15 C 1.1137(2) 0.6299(3) 0.1854(3) 0.0554(7) Uani 1 1 d . . .

H15 H 1.1425 0.5820 0.2539 0.067 Uiso 1 1 calc R . .

C16 C 1.01319(18) 0.6182(2) 0.1212(2) 0.0423(5) Uani 1 1 d . . .

C17 C 0.9560(2) 0.5348(2) 0.1534(2) 0.0436(6) Uani 1 1 d . . .

C18 C 0.9991(2) 0.4532(3) 0.2625(3) 0.0634(8) Uani 1 1 d . . .

H18A H 0.9764 0.4709 0.3354 0.095 Uiso 1 1 calc R . .

H18B H 1.0682 0.4587 0.2875 0.095 Uiso 1 1 calc R . .

H18C H 0.9800 0.3781 0.2338 0.095 Uiso 1 1 calc R . .

C19 C 0.85808(18) 0.5260(2) 0.0823(2) 0.0407(5) Uani 1 1 d . . .

C20 C 0.7978(2) 0.4391(2) 0.1062(3) 0.0518(6) Uani 1 1 d . . .

H20 H 0.8238 0.3874 0.1718 0.062 Uiso 1 1 calc R . .

C21 C 0.7040(2) 0.4295(3) 0.0362(3) 0.0596(7) Uani 1 1 d . . .

H21 H 0.6668 0.3714 0.0539 0.071 Uiso 1 1 calc R . .

C22 C 0.6624(2) 0.5065(3) -0.0630(3) 0.0605(7) Uani 1 1 d . . .

H22 H 0.5980 0.4992 -0.1111 0.073 Uiso 1 1 calc R . .

C23 C 0.7164(2) 0.5916(2) -0.0886(3) 0.0517(6) Uani 1 1 d . . .

H23 H 0.6877 0.6428 -0.1536 0.062 Uiso 1 1 calc R . .

C24 C 0.81551(17) 0.60477(19) -0.0189(2) 0.0395(5) Uani 1 1 d . . .

loop_

 _atom_site_aniso_label

 _atom_site_aniso_U_11

 _atom_site_aniso_U_22

 _atom_site_aniso_U_33

 _atom_site_aniso_U_23

 _atom_site_aniso_U_13

 _atom_site_aniso_U_12

Br1 0.0535(2) 0.0599(2) 0.1064(3) -0.00468(17) 0.01376(18) 0.01510(14)

O1 0.0787(14) 0.0729(13) 0.0357(9) 0.0096(9) 0.0131(9) 0.0298(11)

C1 0.0392(13) 0.0418(14) 0.0641(16) -0.0036(12) 0.0097(12) -0.0020(10)

C2 0.0543(16) 0.0563(16) 0.0547(16) 0.0126(13) 0.0049(13) 0.0077(13)

C3 0.0560(16) 0.0560(16) 0.0404(13) 0.0057(11) 0.0130(11) 0.0052(13)

C4 0.0367(12) 0.0413(12) 0.0395(11) 0.0027(10) 0.0082(10) -0.0041(10)

C5 0.0432(13) 0.0440(13) 0.0364(11) 0.0031(10) 0.0103(10) 0.0007(10)

C6 0.0548(15) 0.0456(14) 0.0347(11) 0.0082(10) 0.0126(11) 0.0028(11)

C7 0.0630(17) 0.0496(15) 0.0353(12) 0.0048(11) 0.0180(11) 0.0059(13)

C8 0.0516(14) 0.0378(12) 0.0327(11) -0.0020(9) 0.0157(10) 0.0070(10)

C9 0.0517(14) 0.0384(12) 0.0343(11) -0.0073(9) 0.0186(10) 0.0015(11)

C10 0.0639(18) 0.0472(15) 0.0508(15) -0.0065(12) 0.0251(13) -0.0053(13)

C11 0.0616(19) 0.066(2) 0.0709(19) -0.0204(15) 0.0313(16) -0.0196(15)

C12 0.0495(16) 0.081(2) 0.0619(18) -0.0260(16) 0.0138(14) -0.0026(16)

C13 0.0543(15) 0.0550(16) 0.0517(15) -0.0077(12) 0.0172(12) 0.0021(13)

C14 0.0475(14) 0.0504(15) 0.0394(12) -0.0001(11) 0.0101(11) 0.0028(11)

C15 0.0505(15) 0.0662(18) 0.0464(14) -0.0129(13) 0.0094(12) 0.0089(14)

C16 0.0489(13) 0.0467(13) 0.0325(11) -0.0079(10) 0.0138(10) 0.0083(11)

C17 0.0587(15) 0.0417(13) 0.0329(11) -0.0001(10) 0.0171(10) 0.0108(12)

C18 0.078(2) 0.0595(17) 0.0476(15) 0.0097(13) 0.0102(14) 0.0133(16)

C19 0.0532(14) 0.0379(12) 0.0372(11) -0.0036(9) 0.0229(11) 0.0049(10)

C20 0.0729(19) 0.0436(14) 0.0465(14) -0.0019(11) 0.0295(13) 0.0008(13)

C21 0.0676(19) 0.0511(16) 0.0701(18) -0.0115(14) 0.0360(16) -0.0131(14)

C22 0.0524(16) 0.0620(18) 0.0674(18) -0.0135(15) 0.0179(14) -0.0035(14)

C23 0.0483(14) 0.0515(15) 0.0540(15) -0.0034(12) 0.0132(12) 0.0053(12)

C24 0.0458(13) 0.0389(12) 0.0362(11) -0.0035(9) 0.0157(10) 0.0063(10)

_geom_special_details

;

All esds (except the esd in the dihedral angle between two l.s. planes)

are estimated using the full covariance matrix. The cell esds are taken

into account individually in the estimation of esds in distances, angles

and torsion angles; correlations between esds in cell parameters are only

used when they are defined by crystal symmetry. An approximate (isotropic)

treatment of cell esds is used for estimating esds involving l.s. planes.

;

loop_

_geom_bond_atom_site_label_1

_geom_bond_atom_site_label_2

_geom_bond_distance

_geom_bond_site_symmetry_2

_geom_bond_publ_flag

Br1 C1 1.892(3) . ?

O1 C5 1.213(3) . ?

C1 C2 1.370(4) . ?

C1 C13 1.380(4) . ?

C2 C3 1.384(4) . ?

C2 H2 0.9300 . ?

C3 C4 1.385(3) . ?

C3 H3 0.9300 . ?

C4 C14 1.385(3) . ?

C4 C5 1.502(3) . ?

C5 C6 1.473(3) . ?

C6 C7 1.328(4) . ?

C6 H6 0.9300 . ?

C7 C8 1.480(3) . ?

C7 H7 0.9300 . ?

C8 C24 1.403(3) . ?

C8 C9 1.406(3) . ?

C9 C10 1.419(4) . ?

C9 C16 1.441(3) . ?

C10 C11 1.351(4) . ?

C10 H10 0.9300 . ?

C11 C12 1.403(5) . ?

C11 H11 0.9300 . ?

C12 C15 1.349(4) . ?

C12 H12 0.9300 . ?

C13 C14 1.374(4) . ?

C13 H13 0.9300 . ?

C14 H14 0.9300 . ?

C15 C16 1.425(4) . ?

C15 H15 0.9300 . ?

C16 C17 1.400(4) . ?

C17 C19 1.405(4) . ?

C17 C18 1.513(3) . ?

C18 H18A 0.9600 . ?

C18 H18B 0.9600 . ?

C18 H18C 0.9600 . ?

C19 C20 1.425(4) . ?

C19 C24 1.434(3) . ?

C20 C21 1.353(4) . ?

C20 H20 0.9300 . ?

C21 C22 1.404(4) . ?

C21 H21 0.9300 . ?

C22 C23 1.357(4) . ?

C22 H22 0.9300 . ?

C23 C24 1.421(4) . ?

C23 H23 0.9300 . ?

loop_

 _geom_angle_atom_site_label_1

 _geom_angle_atom_site_label_2

 _geom_angle_atom_site_label_3

 _geom_angle

 _geom_angle_site_symmetry_1

 _geom_angle_site_symmetry_3

 _geom_angle_publ_flag

C2 C1 C13 120.9(2) . . ?

C2 C1 Br1 120.2(2) . . ?

C13 C1 Br1 118.8(2) . . ?

C1 C2 C3 119.5(2) . . ?

C1 C2 H2 120.3 . . ?

C3 C2 H2 120.3 . . ?

C2 C3 C4 120.9(2) . . ?

C2 C3 H3 119.6 . . ?

C4 C3 H3 119.6 . . ?

C14 C4 C3 118.2(2) . . ?

C14 C4 C5 117.9(2) . . ?

C3 C4 C5 124.0(2) . . ?

O1 C5 C6 121.4(2) . . ?

O1 C5 C4 119.0(2) . . ?

C6 C5 C4 119.61(19) . . ?

C7 C6 C5 124.8(2) . . ?

C7 C6 H6 117.6 . . ?

C5 C6 H6 117.6 . . ?

C6 C7 C8 127.9(2) . . ?

C6 C7 H7 116.0 . . ?

C8 C7 H7 116.0 . . ?

C24 C8 C9 119.9(2) . . ?

C24 C8 C7 121.0(2) . . ?

C9 C8 C7 119.0(2) . . ?

C8 C9 C10 121.3(2) . . ?

C8 C9 C16 119.9(2) . . ?

C10 C9 C16 118.8(2) . . ?

C11 C10 C9 121.3(3) . . ?

C11 C10 H10 119.4 . . ?

C9 C10 H10 119.4 . . ?

C10 C11 C12 120.4(3) . . ?

C10 C11 H11 119.8 . . ?

C12 C11 H11 119.8 . . ?

C15 C12 C11 120.4(3) . . ?

C15 C12 H12 119.8 . . ?

C11 C12 H12 119.8 . . ?

C14 C13 C1 119.0(2) . . ?

C14 C13 H13 120.5 . . ?

C1 C13 H13 120.5 . . ?

C13 C14 C4 121.6(2) . . ?

C13 C14 H14 119.2 . . ?

C4 C14 H14 119.2 . . ?

C12 C15 C16 122.2(3) . . ?

C12 C15 H15 118.9 . . ?

C16 C15 H15 118.9 . . ?

C17 C16 C15 122.9(2) . . ?

C17 C16 C9 120.2(2) . . ?

C15 C16 C9 116.9(2) . . ?

C16 C17 C19 119.6(2) . . ?

C16 C17 C18 120.6(2) . . ?

C19 C17 C18 119.8(2) . . ?

C17 C18 H18A 109.5 . . ?

C17 C18 H18B 109.5 . . ?

H18A C18 H18B 109.5 . . ?

C17 C18 H18C 109.5 . . ?

H18A C18 H18C 109.5 . . ?

H18B C18 H18C 109.5 . . ?

C17 C19 C20 122.0(2) . . ?

C17 C19 C24 120.5(2) . . ?

C20 C19 C24 117.5(2) . . ?

C21 C20 C19 122.0(3) . . ?

C21 C20 H20 119.0 . . ?

C19 C20 H20 119.0 . . ?

C20 C21 C22 120.4(3) . . ?

C20 C21 H21 119.8 . . ?

C22 C21 H21 119.8 . . ?

C23 C22 C21 119.9(3) . . ?

C23 C22 H22 120.1 . . ?

C21 C22 H22 120.1 . . ?

C22 C23 C24 121.9(3) . . ?

C22 C23 H23 119.1 . . ?

C24 C23 H23 119.1 . . ?

C8 C24 C23 121.9(2) . . ?

C8 C24 C19 119.8(2) . . ?

C23 C24 C19 118.3(2) . . ?

_diffrn_measured_fraction_theta_max   0.981

_diffrn_reflns_theta_full   30.34

_diffrn_measured_fraction_theta_full   0.981

_refine_diff_density_max   0.931

_refine_diff_density_min   -0.825

_refine_diff_density_rms   0.060